

SUCROSE CRYSTALLINITY QUANTIFICATION USING FTIR SPECTROSCOPY

MASTERS THESIS  
SUBMITTED TO THE FACULTY OF THE GRADUATE SCHOOL  
OF THE UNIVERSITY OF MINNESOTA  
BY

AIMEE KWONG MORTENSON

IN PARTIAL FULFILLMENT OF THE REQUIREMENTS FOR  
THE DEGREE OF MASTER OF SCIENCE

CO-ADVISOR: CHRISTINE NOWAKOWSKI  
CO-ADVISOR: BARAEM ISMAIL

OCTOBER 2014



## **Acknowledgments**

I wish to express my gratitude to my co-advisors Dr. Baraem Ismail and Dr. Christine Nowakowski for their guidance, support, and expertise. I would not be the scientist I am today without both of their influences on my success and motivation over the years. My history of food science started in Dr. Ismail's University of Minnesota lab, and I thank her for taking me into her lab as both an undergraduate while finishing my chemistry degree and now as a Master's student. This research opportunity was a true testament of Dr. Nowakowski's strive for creativity in science and her passion for finding interesting research topics. I owe recognition and gratitude to General Mills Inc. for providing me with the support needed to complete my graduate degree. I would also like to thank my committee members Drs. Dave Smith and Michelle Driessen for accepting the challenge of evaluating my thesis.

I would also like to thank my good friends Cherry Wang, Brian Folger, Jordan Walter, Kirsten Ruud, Kristina Jung, and Lauren Gillman for being such great lab mates and forever friends. The reason I had a great graduate school experience was because of the wonderful relationships I had built over the years. A special thanks to Tim Peters and Jody Panchyshyn for their help throughout the trials and tribulations of my research.

Words cannot adequately express my love and gratitude towards my family and close friends for their support, encouragement, and for understanding my ambition towards perfection. I wish to express gratitude towards my Aunt Anita for being my rock and my role model over the years; our relationship has made me the person I am today. Last but not least, a special thank you to Brad for always being by my side and for helping me make my dreams come true.

*I dedicate my thesis to my nieces and nephews as an example of what hard work can get you. I also dedicate this to my Husband Brad and my Aunt Anita, who supported me each step of the way.*

## **Abstract**

Understanding sucrose crystallinity is important especially as the food industry has reduced sugar content in products. Robust quantification methods determine crystallinity effects from formulation and/or processing changes. Differential Scanning Calorimetry (DSC) quantifies crystallinity within products, albeit requiring sample destruction. Fourier Transform Infrared (FTIR) spectroscopy can quantify different materials and has the potential of mapping crystallizing areas within a complex food matrix. Additionally, this method can be used to quantify sucrose crystallinity by a non-destructive, rapid means.

Currently the methods used to quantify for sucrose crystallinity have been explored in pharmaceutical, lower moisture systems, where complex food matrices are not a factor. The objectives were to create a FTIR method to quantify the amount of crystalline sucrose in mixtures at various concentrations and to determine feasibility of spatial analysis capabilities using FTIR microscope methods.

The development of the method was built using model systems of sucrose and carbohydrate blends. Crystallinity was measured via both FTIR and DSC. Samples were freeze-dried and held at different humidity levels to determine which IR peaks were independent of moisture content. IR spectral peaks that correlated best with the DSC measured sucrose crystallinity content were identified. Different calibration methods were concurrently used to obtain the best statistical fit using TQ Analyst® software. FTIR spatial analyses were performed on samples to assess feasibility of the method and commercialized baking mixes were tested to determine efficacy of the bulk method on complex food matrices.

Three regions of interest ( $1087\text{ cm}^{-1}$ ,  $991\text{ cm}^{-1}$ , and  $909\text{ cm}^{-1}$ ) were found to have the best Partial Least Squares (PLS) correlation to the crystallinity percentage. A Performance Index of 96.3 and a Root Mean Square Error of Prediction 0.925

were achieved with the three regions. These results show the potential of a robust method to quantify heterogeneous microdomains within foods, without interference from complex matrices. The three regions were statistically comprehensive at defining the variables as a bulk method. The spatial analysis using the FTIR microscope was affected by sucrose orientation, beam intensity, and shifts in peaks. A lower magnification spatial method would be a more applicable use of this method in an inline FTIR technology. The future application of this technology is to combine observed microdomains and correlate them to events such as stickiness or drying rates, for example.

## Table of Contents

<b>Acknowledgments</b> .....	<b>i</b>
<b>Abstract</b> .....	<b>iii</b>
<b>List of Tables</b> .....	<b>vii</b>
<b>List of Figures</b> .....	<b>ix</b>
<b>1. Review of Literature</b> .....	<b>1</b>
1.1. Introduction and Objectives .....	1
1.2. Crystalline Sucrose .....	4
1.3. Stickiness and Adhesion.....	6
1.4. Historical Material Characterization for Crystalline and Amorphous Sucrose .....	8
1.4.1. Chemometrics.....	10
1.4.2. Differential Scanning Calorimetry.....	14
1.4.3. Microscopy.....	15
1.4.4. X-Ray Diffraction .....	16
1.4.5. Nuclear Magnetic Resonance Spectroscopy.....	17
1.4.5. Infrared Spectroscopy.....	18
1.4.6. Raman Spectroscopy.....	18
1.4.7. Near-Infrared Spectroscopy.....	19
1.4.8. Mid-Infrared Spectroscopy .....	20
1.4.9. FTIR Microscopy.....	24
1.5. Conclusion.....	25
<b>2. Materials and Methods</b> .....	<b>26</b>
2.1. FTIR and DSC Settings .....	26
2.2. Methods for Sample Preparation .....	27
2.2.1. Sample Preparation Using Nujol as a Medium .....	27
2.2.2. Sample Preparation Using 63DE Corn Syrup as a Medium.....	28
2.2.3. Sample Preparation Using 10DE Maltodextrin as a Medium .....	29
2.3. Methods for Analysis of Spectra .....	29
2.3.1. Analysis of FTIR Spectrum of 10DE and Sucrose.....	29
2.3.2. Moisture of 10DE Maltodextrin and the Effects on the Mixture.....	33

2.3.3. Evaluation of Peaks from Experiment 2.3.2.....	36
2.4. Calibration Curve Methods.....	40
2.4.1. Calibration Curve Experiment to Determine Peak(s) of Interest.....	40
2.4.2. Partial Least Squared Method Development.....	42
2.5. Applications of Sucrose Crystallinity Quantification Method in Food Products.....	42
2.6. Methods for FTIR Microscope.....	43
2.6.1. FTIR Image Using FTIR Microscope.....	43
2.6.2. Intrinsic Factor - Effect of Crystal Size.....	43
<b>3. Results and Discussion.....</b>	<b>45</b>
3.1. Sampling System for FTIR apparatus Determination.....	45
3.2. Effect of Using Nujol and 63DE for Quantification Method Medium.....	45
3.3. Sucrose Crystallinity Quantification of 10DE Maltodextrin and Sucrose using DSC.....	46
3.4. Bulk method of 10DE Maltodextrin and Sucrose Quantification Method.....	48
3.5. Analysis of Commercialized Cake Mixes.....	52
3.6. The Difference between Bulk and Spatial FTIR.....	53
3.7. Crystal Size Effect on the FTIR Microscope Image.....	59
3.8. Sucrose and 10DE Maltodextrin Mixtures Analyzed by the FTIR Microscope Method.....	60
<b>4. Conclusions, Implications, and Recommendations.....</b>	<b>63</b>
<b>5. References.....</b>	<b>64</b>
<b>Appendix A: Cake Mix Ingredient Information.....</b>	<b>69</b>



## List of Tables

<i>Table 1: Composition of sucrose and Nujol mixtures used in the first FTIR experiment to determine if Nujol would be the proper medium to build a quantification method. ....</i>	<i>28</i>
<i>Table 2: Composition of sucrose and 63DE corn syrup mixtures analyzed using FTIR to determine if 63DE was appropriate to use as a method medium .....</i>	<i>28</i>
<i>Table 3: Composition of 10DE maltodextrin and sucrose mixtures evaluated using DSC and FTIR. ....</i>	<i>29</i>
<i>Table 4: Regions of FTIR spectra evaluated using the peak intensity ratio analysis at different levels of sucrose with corresponding FTIR interpretation. ...</i>	<i>40</i>
<i>Table 5: Regions of FTIR spectra evaluated using the peak intensity ratio analysis at different levels of sucrose. ....</i>	<i>40</i>
<i>Table 6: Different PLS combinations performed to determine which was most effective at quantifying sucrose crystallinity.....</i>	<i>42</i>
<i>Table 7: The measurement of percent crystallinity of sucrose mixtures with 10DE maltodextrin determined by DSC.....</i>	<i>48</i>
<i>Table 8: Number of spectra culled using TQ Analyst® software at each concentration and region to achieve the performance indexes in Table 9.....</i>	<i>49</i>
<i>Table 9: Performance Index determined by TQ Analyst® at regions found using sucrose and maltodextrin mixtures at different concentrations and analyzed using FTIR. ....</i>	<i>50</i>
<i>Table 10: PI values of different combinations of regions chosen based on PI and RMSEP values of statistical models from Table 8. ....</i>	<i>51</i>

*Table 11: Baking mix sucrose results determined by AOAC method and % sucrose crystallinity by DSC along with FTIR % sucrose crystallinity results..... 52*

## List of Figures

<i>Figure 1: Sucrose molecular structure (Linstrom &amp; Mallard, 2013).....</i>	<i>5</i>
<i>Figure 2: Comparison of arrangement of crystals between a crystalline, polycrystalline, and amorphous structure. ....</i>	<i>6</i>
<i>Figure 3: State diagram of sucrose (Chen, 2013).....</i>	<i>8</i>
<i>Figure 4: A systematic evaluation of data to perform proper chemometrics for method development (Beebe et al., 1998).....</i>	<i>11</i>
<i>Figure 5: Dispersive spectrometer diagram (Thermo Nicolet Corporation, 2002) .....</i>	<i>21</i>
<i>Figure 6: Michelson Interferometer Diagram (Thermo Nicolet Corporation, 2002) .....</i>	<i>22</i>
<i>Figure 7: Smart Diffuse Reflectance Accessory with Sample Cup Example .....</i>	<i>26</i>
<i>Figure 8: Nujol FTIR spectrum (Linstrom &amp; Mallard, 2013) .....</i>	<i>27</i>
<i>Figure 9: Peak intensity ratio analysis performed around 1090 cm<sup>-1</sup> of 100% and 50% sucrose with 10DE maltodextrin and 100% 10DE maltodextrin sample .....</i>	<i>30</i>
<i>Figure 10: Peak intensity ratio analysis performed around 900 cm<sup>-1</sup> of 100% and 50% sucrose with 10DE maltodextrin and 100% 10DE maltodextrin sample .....</i>	<i>31</i>
<i>Figure 11: Peak intensity ratio analysis performed around 1100 cm<sup>-1</sup> of 100% and 50% sucrose with 10DE maltodextrin and 100% 10DE maltodextrin sample .....</i>	<i>32</i>
<i>Figure 12: Peak intensity ratio analysis performed around 3500 cm<sup>-1</sup> of 100% and 50% sucrose with 10DE maltodextrin and 100% 10DE maltodextrin sample .....</i>	<i>33</i>

*Figure 13: Sucrose at 25% concentration with maltodextrin was evaluated using FTIR bulk method on both the freeze dried sample and sample at 6.0% moisture. .... 34*

*Figure 14: Sucrose at 50% concentration with maltodextrin was evaluated using FTIR bulk method on both the freeze dried sample and sample at 3.6% moisture. .... 35*

*Figure 15: Sucrose at 0% concentration with maltodextrin was evaluated using FTIR bulk method on both the freeze dried sample and sample at 7.6% moisture. .... 35*

*Figure 16: Sucrose at 100% concentration was evaluated using FTIR bulk method on both the freeze dried sample and sample at 0.16% moisture. .... 36*

*Figure 17: Peak intensity ratio analysis performed around 2925 cm<sup>-1</sup> of 100% and 50% sucrose with 10DE maltodextrin and 100% 10DE maltodextrin sample. Peak analysis was determined by experiment 2.3.2. .... 37*

*Figure 18: Peak intensity ratio analysis performed around 1575 cm<sup>-1</sup> of 100% and 50% sucrose with 10DE maltodextrin and 100% 10DE maltodextrin sample. Peak analysis was determined by experiment 2.3.2. .... 38*

*Figure 19: Peak intensity ratio analysis performed around 1175 cm<sup>-1</sup> of 100% and 50% sucrose with 10DE maltodextrin and 100% 10DE maltodextrin sample. Peak analysis was determined by experiment 2.3.2. .... 39*

*Figure 20: An example window of a mapped surface where scans from the FTIR were taken at each point. .... 44*

*Figure 21: Example of sucrose (squares) and Nujol (shaded area) mixture with incoming incident of light entering and leaving the surface of the Nujol versus the entire sample. .... 46*

*Figure 22: A example DSC thermogram of 100% analytical grade sucrose with a delta H of 125.6 J/g which was used to calculate the concentration of sucrose crystallinity of a bulk sample..... 47*

*Figure 23: The PLS quantification method calibration curve of 1087, 991, and 909 cm<sup>-1</sup> regions. The calibration set were the observations used and the validation set was used to calculate the RMSEP values. .... 51*

*Figure 24: Right side represents the bulk sample measurement where the multiple incidents of light occur along with a larger amount of diffuse reflectance that is reflected back into the detector. The left side represents the FTIR microscope sample measurement where the aperture is smaller and therefore has a smaller amount of light reflected back to the detector..... 53*

*Figure 25: An image of the total surface of 100% 10DE maltodextrin where the location of the 2 x 2 map taken at a (x, y) of approximately (14900 – 15150, 6550 – 6800). Microscope method spectra of a single point in comparison to the bulk method of 100% 10DE maltodextrin ..... 55*

*Figure 26: A 100% sucrose sample where the location of the 2 x 2 map taken at a (x, y) of approximately (5500 – 5750, 3500 – 3750). Microscope method spectra of a single point in comparison to the bulk method of sucrose..... 57*

*Figure 27: 10DE maltodextrin and sucrose quantified using the FTIR microscope spectra..... 58*

*Figure 28: Particle size distribution of analytical grade sucrose with d(0.5) = 368.5 μm ..... 59*

*Figure 29: Particle size distribution of powdered sucrose with d(0.5) = 96.6 μm 59*

*Figure 30: Predicted values of percent crystallinity of powdered and analytical grade sucrose..... 60*

*Figure 31: The FTIR microscope samples were plotted to show the regression shift between the bulk method and the microscope method. Also the intensity variability was more pronounced with the sucrose samples than with the maltodextrin samples..... 61*

## **1. Review of Literature**

### **1.1. Introduction and Objectives**

Sugar consumption has increased between 1950 and 2000 by 39%, which results in the average American consuming around three pounds of sugar each week or up to 16% of their total daily calories (USDA, 2014; J. Wilson, 2014). Therefore, reduction of intake of calories from added sugars in the diet has been recommended from expert groups such as the American Heart Association, American Academy of Pediatrics, and the World Health Organization (USDA, 2014). Changes in the nutrition facts label are proposed to inform the consumer about the amount of added sugars versus the current label of overall sugars (i.e. naturally occurring and added sugars) in a product (USDA, 2014). With increased visibility of added sugars on the label, other ingredients such as aspartame, an intense sweetener, and xylitol, a sweet bulking agent, have increased use in the food industry to build back sweetness and mass in a food product. These options offer calorie reduction on the label, but does not aid in sucrose crystallinity, an important attribute in food production.

Sucrose reduction can pose many different problems in food products. Sucrose crystallinity is affected by lower concentration (70 – 76% w/w) of sucrose which can lead into other issues such as stickiness and other organoleptic changes in the finished product (Ben-Yoseph et al., 2000). Stickiness is observed at higher moisture content and when sucrose is in an amorphous state. Low sucrose crystallinity in processed food can present risks such as clumping of product, which reduces flowability of a product through a continuous dryer and sticking product to dryer walls which would be difficult to clean. In packaging, clumping can cause uneven weight distribution and imprecise product delivery into a container. Over time, clumping can also occur within a container which causes product to create a solid mass, which is not easily pourable and could result in not meeting consumer expectations of the product.

The eating experience for consumers can change with different levels of crystalline sucrose. The appearance of food products with high sucrose crystallinity may have frosty to matte appearance whereas low sucrose crystallinity may have gloss appearance. For example, fudge, fondant, and other crystalline confections have a higher crystalline content of sucrose when compared to hard candies (Chen, 2013; Lee, 2010). In addition to appearance, flavor can change in food products with different levels of sucrose crystallinity. Since crystalline sucrose dissolves slower than amorphous sucrose, early sensory research has determined that it reduces overall sweetness perception (Gianfrancesco et al., 2012). Sucrose reduction research is the balance of how sucrose crystallinity can affect these different attributes and the magnitude of these attributes on other characteristics of the finished product.

Currently, Differential Scanning Calorimetry (DSC), a thermoanalytical technique, is commonly used to measure the amount of both crystalline and amorphous sucrose in food. This primary, or direct, measurement method measures the temperature and heat flow associated with phase transition in materials as a function of time and temperature. The concentration of sucrose crystallinity is determined through calculation of different DSC responses, and the value is a concentration of the overall product. DSC is effective at measuring for sucrose phases, but since the system measures a sample as a whole it is not surface sensitive and destroys the sample in the process (Lehto et al., 2006). The bulk measurement sample preparation for the DSC is a disadvantage of the analysis; this limits the understanding of spatial analysis of a sample surface.

A robust quantification method will expand research and development knowledge by identifying sucrose crystallinity effects from different formulation and processing conditions. Fourier Transform Infrared Spectroscopy (FTIR) provides information on molecular structure and intermolecular interactions within the food matrices. FTIR mapping has been used in a variety of ways such as to evaluate the surfaces of old master paintings to discriminate paints of the same color from



each other such as different hues or origins of a red color (Muehlethaler et al., 2011). The pharmaceutical industry uses spectroscopy to identify and quantify attributes such as compound distribution in a solid formed drug (crystalline or amorphous), which is essential for bioavailability for example (Stephenson et al., 2001). Spectral mapping technology of food surfaces have been done to analyze for carotenoid content, but little work exists overall on the application capabilities to food.

Enabling FTIR spectroscopy as a method to quantify for sucrose crystallinity in food can also enable a spatial analysis using similar methodologies. Different apparatus such as the FTIR microscope and other handheld devices have capabilities for inline testing in food production plants. This research will develop a foundation of knowledge of using the FTIR to analyze for sucrose crystallinity. Sucrose formulation changes can affect the overall texture, processability, and sweetness. As the food industry introduces small changes in formulas or processing changes in food products, it is essential to develop a method to characterize and quantify sucrose crystallinity on these heterogeneous surfaces. As methodology develops for sucrose crystallinity, more methods can be eventually developed for other food products, focusing on different food attributes and packaging.

Therefore, the specific objectives of this research were:

1. To develop a non-destructive, rapid method to quantify crystalline sucrose in model food systems by FTIR spectroscopy.
2. To test the feasibility of FTIR mapping.

Hypotheses include:

1. A FTIR calibration curve, created using DSC information, can aid in the quantification of crystalline sucrose
2. Using the data from the FTIR research, an imaging method using FTIR microscopy can be used to quantify crystalline sucrose spatially.

## **1.2. Crystalline Sucrose**

Sucrose is one of the most widely used disaccharides in foods, biomaterials, and pharmaceuticals (Noel et al., 2000). Sucrose is an organic compound that appears in nature in different forms, i.e., crystalline and amorphous, and it is obtained from sugar cane or sugar beets. In 2011, 168 million metric tons of table sugar (sucrose) was produced world-wide (USDA, 2011). In food, sucrose plays an important role in providing sweet taste and specific textural properties (Chen, 2013). Crystallization and glass transition are important in foods as it plays a critical role in shelf life, quality, and texture. In supersaturated aqueous solutions, sucrose crystallizes (Mathlouthi et al., 1996).

Carbohydrates are present in almost all foods as sugars, starches, and fiber and may exist as crystalline compounds, semicrystalline compounds, or totally amorphous compounds (Y. Roos, 1995). Sugar is a carbohydrate, occurring in many vegetables, fruits, and dairy foods. Sucrose consists of equal parts of glucose and fructose (simple sugars or monosaccharides) joined by an ether bond to create a disaccharide. Sucrose is a disaccharide composed of the monosaccharide glucose and fructose which forms the molecular formula:

( $C_{12}H_{22}O_{11}$ ). The glucose six member ring and the fructose five member ring are joined by an acetal oxygen in the alpha position.

Structure of a sucrose molecule is shown in Figure 1. In crystalline form, sucrose forms lattices that are composed of an ordered layering of molecules. The ordering is dependent on the nature of the forces and interactions among molecules. In sucrose, the molecules are arranged in a well-defined pattern within the lattice that makes up a crystal. Within sucrose crystals, weak molecular forces or hydrogen bonds occur to create a crystal lattice. Molecular arrangement within a crystal can differ on different faces of the crystal. Slight differences in these conformations can impact physical properties and growth characteristics (Richard W Hartel et al., 2011).

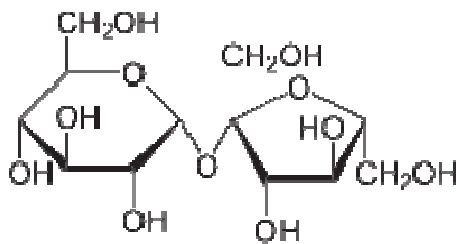


Figure 1: Sucrose molecular structure (Linstrom & Mallard, 2013)

Variations in sucrose come from the following attributes: a) origin, b) impurity, c) polymorphism (or allotrophism), d) superheating, e) liquefaction, and f) thermal decomposition in addition to melting (Lee, Thomas, Jerrell, et al., 2011). The different sources (e.g., cane and beet) and manufacturing (e.g., reagent grade vs. commercial grade) are parts of different origins which can introduce different melting temperatures (Lee, Thomas, & Schmidt, 2011b). Since differences such as the origin can change the melting temperature of sucrose, analyses to quantify sucrose crystallinity such as DSC which depends on melting temperature could be affected by the variation in measurement (Lee, Thomas, & Schmidt, 2011b; Lee, Thomas, Jerrell, et al., 2011).

In addition to attributes listed, glucose and fructose can also alter sucrose crystalline structure by changing its shape, which can vary the response depending on the type of analysis (Sgualdino et al., 1998). The morphology has shown to change with high concentrations of invert sugar, which is a 1:1 molecular ratio of glucose and fructose produced by hydrolysis of the 1,6 bond in industrial plants (Smythe, 1967). Furthermore, certain sites on a sucrose crystal are prone to structure alteration from glucose and fructose which can cause kinks in the crystal structure and also crystal growth patterns (Sgualdino et al., 1996). These changes in structure are measured and detected by different methods, but can alter a quantification and/or qualification method without a robust calibration or understanding of the variation.

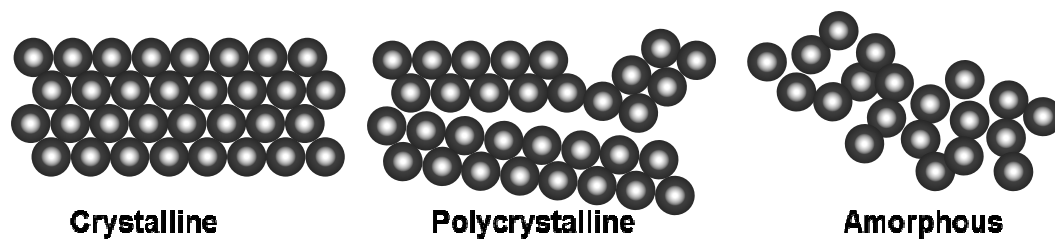


Figure 2: Comparison of arrangement of crystals between a crystalline, polycrystalline, and amorphous structure.

Structural changes in crystalline sucrose produce different attributes (Figure 2). Crystalline structure has an organized lattice structure whereas an amorphous structure has a high amount of disorganization. A polycrystalline structure possesses both crystalline and amorphous structures where the crystal lattice has parts of disorganization. Different levels of stickiness and adhesion properties of food products with sucrose are affected by these structural differences (Nowakowski & Hartel, 2002).

### **1.3. Stickiness and Adhesion**

The two most common problems limiting shelf life in hard candies are crystallization and stickiness (Cotton et al., 1955; Nowakowski, 2000). Not only

do changes occur structurally, like ones mentioned in the previous section, but the changes in morphism in sucrose can affect macro scale such as stickiness and adhesion. According to Nowakowski and Hartel, stickiness is the manifestation of the adhesive properties of a substance, where cohesion is the force within a material and adhesion is the force between materials. Amorphous sugar products and its stability depend on sugar type, water content, and storage conditions such as temperature and relative humidity (Nowakowski & Hartel, 2002).

Attributes such as increasing stickiness change as a function of increasing moisture until an optimal is reached and further moisture can reduce stickiness (Nowakowski & Hartel, 2002). Water changes glass-transition-controlled variations in food structures such as stickiness (Y. H. Roos, 1998). The glass transition temperature ( $T_g$ ) is the midpoint of the glass transition zone which is the temperature range where a sugar glass loses solid-like characteristics and begins to flow (Nowakowski & Hartel, 2002).

Glass transition is kinetically controlled, but the fundamental interactions for transition are based on equilibrium. The conditions of equilibrium are described by phase diagrams where phase/state expectations are defined depending on food products (Hartel et al., 2011). The phase diagram shown in Figure 3 estimates the glass or crystalline state of the sucrose-water binary mixture based on the amount of cross-linking, molecular weight, and diluent content on  $T_g$  (Chen, 2013).

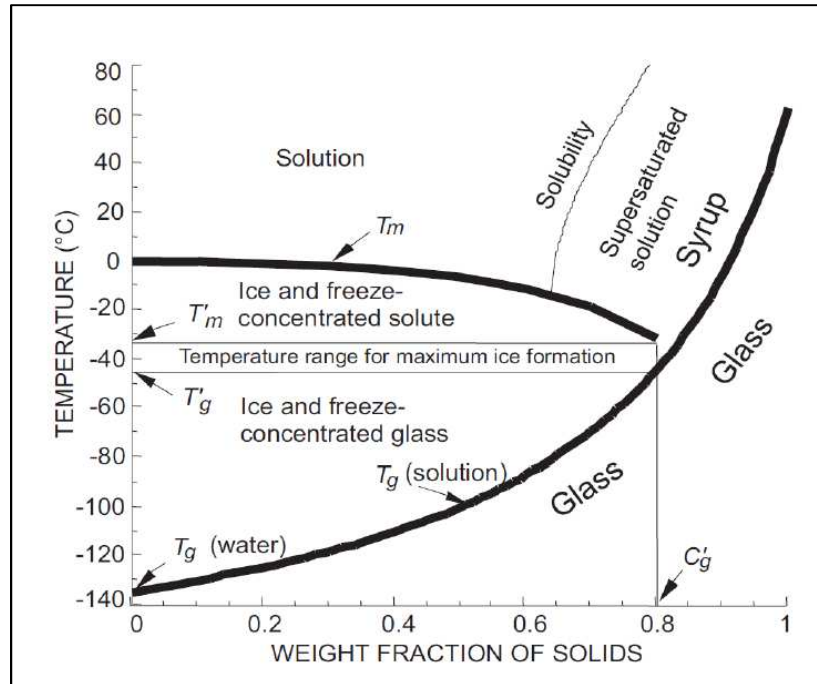


Figure 3: State diagram of sucrose (Chen, 2013)

#### 1.4. Historical Material Characterization for Crystalline and Amorphous Sucrose

According to Roos, phase and state transitions in solid food matrices have traditionally been studied using Differential Scanning Calorimetry (DSC) (Roos, 1995). Crystalline sucrose and food structure analysis has also been measured using microscopy and X-Ray Diffraction (XRD). Microscopy was initially used to determine if adulteration of foods as present or if there was a contaminant (Kaláb et al., 1995). More recently, microscopy has been used to evaluate food structure such as crystallinity in addition to XRD. Procedures using XRD to estimate crystallinity are based on the measurement of X-ray scattering from the entire sample including the amorphous region of the sample (Shah et al., 2006). These methods directly measure for crystalline sucrose whereas other spectroscopic techniques quantitatively measure for crystalline sucrose indirectly.

Spectroscopic techniques can be used in conjunction with solid-state techniques such as microscopy, DSC, and XRD (Shah et al., 2006). Techniques such as Fourier Transform Infrared Spectroscopy (FTIR) reflect significant spectral differences between crystalline and amorphous phases as vibrational bands and intensity are directly proportional to the concentration of the crystalline phase (Shah et al., 2006). Other spectroscopy techniques include Near Infrared Spectroscopy (NIR), Raman Spectroscopy, and Nuclear Magnetic Resonance Spectroscopy (NMR).

The XRD technique measures the differences of atoms in crystals whereas FTIR, NIR, and Raman techniques measure the bond and lattice bending and stretching vibrations (Stephenson et al., 2001). NIR has been used to measure crystalline materials in pharmaceutical analysis and is also nondestructive and require no sample preparation (Shah et al., 2006). In the food industry, NIR has been used to monitor dairy composition and analyze grain varieties (Driver & Didona, 2009).

According to Pellow-Jarman, et al. crystal powder quantification is difficult to reproduce, but Raman spectroscopy research to quantify for potassium chromate has found promising results with further refinement (Pellow-Jarman et al., 1996). Other Raman spectroscopy applications in food included grain composition and quantifying carotenoid content in several systems including Atlantic salmon (Smith & Dent, 2005). NMR measures the electronic environments of nuclei and has been used to measure pharmaceutical solids which is beneficial because of its superior spectral resolution (Stephenson et al., 2001).

A simple linear regression model is used commonly with DSC, microscopy, and XRD methods. The model (Equation 1) indicates that there is only one independent variable ( $x$ ) to predict the dependent variable ( $y$ ), therefore simple. The linearity comes from the linear relationship between  $\beta_0$  and  $\beta_1$  (Rencher & Schaalje, 2007).

$$y_i = \beta_0 + \beta_1 x_1 \quad (\text{Equation 1})$$

In comparison, the multiple regression model (Equation 2) uses the basis of the simple linear regression but instead of one independent variable the linear relationship would be with several independent variables (Rencher & Schaalje, 2007).

$$y_i = \beta_0 + \beta_1 x_1 + \beta_2 x_2 + \dots + \beta_k x_k \quad (\text{Equation 2})$$

Multiple linear regression models are commonly used in spectroscopy where the different independent variables would be different peaks or regions and the response would be percent crystallinity.

#### **1.4.1. Chemometrics**

In experimental life sciences such as chemistry, chemometrics is used to analyze chemical data by statistical and mathematical techniques (Beebe et al., 1998). More importantly, Beebe, et. al, expanded on the aforementioned general definition of chemometrics to a broader definition of chemometrics as the entire process whereby data (e.g., numbers in a table) are transformed into information used for decision making. As analysis types grew in complexity throughout the 1980s to the 1990s, with higher volume of information to cull in order to determine pertinent information, chemometrics was a key ingredient in the data mining necessary to find solutions to data analysis problems (Brereton, 2007).

The reason to design statistical experiments in chemistry is to screen, optimize, save time, and/or enable quantitative modeling.



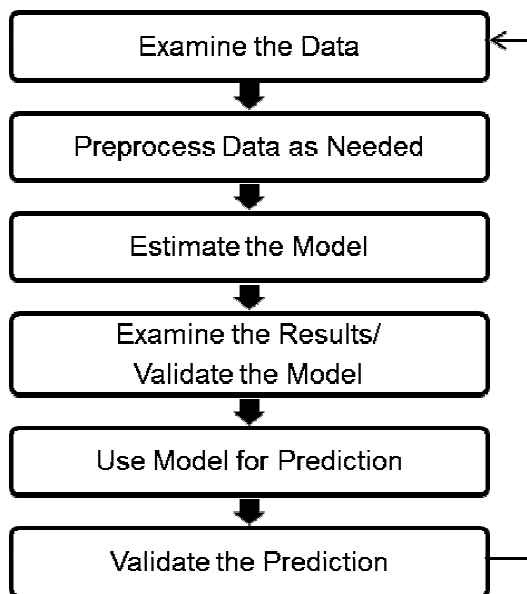


Figure 4: A systematic evaluation of data to perform proper chemometrics for method development (Beebe et al., 1998).

To build a systematic evaluation of data independent of the method, several steps must be taken to perform proper chemometrics (See Figure 4); part of the evaluation of data includes the analysis after the initial method development. When the validation of the prediction does not perform with a high correlation, further examination of the data is needed before the method is considered finished. Partial Least Squares (PLS), a form of multivariate calibration and prediction, is commonly used in different chromatographic and spectroscopic quantitative models, where the principle behind the method is to consider the importance of both modelling the concentration information and modelling the experimental information (Brereton, 2007). By using PLS, it is possible to analyze multiple components simultaneously. PLS assumes that there are errors in both the concentration used in the calibration due to errors such as in dilution and weighing, and also the spectra or chromatograms.

Other univariate and multivariate statistical approaches such as Beer's Lambert Law and Classical Least Squares (CLS) are other types of analysis which can be also used to analyze for attributes such as peaks in a spectra (Brereton, 2007).

Beer's Law is suitable for a quantification of a single component sample. Depending on which peaks are chosen to correlate with the concentration of sucrose crystallinity, it could be a single peak which best represents said attribute or a combination of peaks or components which best quantify for sucrose crystallinity. A simple multivariate technique such as CLS is an expanded Beer's Law, where the components are considered on a linear model of all species that are known (Mark & Workman, 2010). The disadvantage of using this method is that the relationship of the component to the concentration is linear, which is attribute dependent. Also for CLS modelling, if a substance appears in the sample which was not used in the initial build of the model, the model will fail its predictions. In terms of sucrose crystallinity and the robustness of the methodology, it is imperative to build the foundation of the method based on a robust model which can ignore unknown substances such as other ingredients or different matrices.

Prediction error of the calibration or the 'training' set is reduced the higher the amount of components or spectra (Brereton, 2007). The caveat of choosing high amounts of spectra to achieve a lower prediction error is noise. Noise can introduce artifacts or unknowns into the sample set. Several spectra can be used to start the process to build the PLS method. Culling data during the build of the calibration is part of the process where the spectra that introduce error and/or noise are removed from the quantification method. Simultaneously, spectra are chosen to remain in the PLS method as part of the calibration set or part of the validation set. Validation set of spectra are designed to teach the methodology of which spectra outside of the calibration set are used to validate a prediction model.

The PLS method encompasses Principle Component Analysis (PCA) methodology for screening data where data is screened using in-effect for correlations, and each successive correlation being a factor. Essentially the PLS method is built using an algorithm where a regression of percent sucrose

crystallinity (Equation 3) is on the latent variables (Equation 4) which is a linear combination of peaks (predictor variables) (Brereton, 2007; Stefan, 2006).

The following equations are a simplified form of the non-linear iterative partial least squares (NIPALS) algorithm (Stefan, 2006). Equation 3 is the more general response of percent sucrose crystallinity on the latent variables.

$$y_i = \beta_0 + \beta_1 L_1 + \beta_2 L_2 + \dots + \beta_n L_n \text{ (Equation 3)}$$

In these equations, n denotes the number of peaks chosen to be used to define the response. Equation 4 is comprised of a series of components which represent the linear combinations of peaks where a, b, and c represent the coefficients from the NIPALS algorithm and x represents the predictor variables or the peaks in this research. Depending on the number of predictor variables the number of PLS components can increase.

$$\begin{aligned} L_1 &= a_1 x_1 + a_2 x_2 + a_3 x_3 + \dots + a_n x_n && \text{1}^{\text{st}} \text{ PLS component} \\ L_2 &= b_1 x_1 + b_2 x_2 + b_3 x_3 + \dots + b_n x_n && \text{2}^{\text{nd}} \text{ PLS component} \\ L_3 &= c_1 x_1 + c_2 x_2 + c_3 x_3 + \dots + c_n x_n && \text{3}^{\text{rd}} \text{ PLS component} \\ &\vdots && \end{aligned} \quad \text{(Equation 4)}$$

The PLS method has shown to predict well in the presence of unknown constituents within a sample (Mark & Workman, 2010). Ideally this is the model or method of choice, because it provides an accurate and robust prediction in the presence of different food constituents such as different dextrans or sweetness enhancers or different food matrices such as bakery items, candies, or cereal coatings. The PLS method is computationally very fast compared to other methods and allows to have less calibration spectra (observations) than peaks (explanatory variables) to build a quantification method (Stefan, 2006). In a CLS or multiple linear regression the variables would need to be collinear whereas PLS would not. This allows for more flexibility when building a calibration curve because PLS does not require many observations or collinear variables.

### 1.4.2. Differential Scanning Calorimetry

Differential Scanning Calorimetry (DSC) is a thermo-analytical technique which directly measures the physical and chemical changes that happen in a material as a function of temperature (Chen, 2013). This technique documents the melting profile of the crystals in a food sample within the calorimeter. Phase transitions are often categorized according to first-order, second-order, or higher-order transitions (Y. Roos, 1995). Glass transition temperature ( $T_g$ ), is used to define the physical state of different materials (Slade & Levine, 1991). A second order phase transition temperature is defined by  $T_g$  at which the a solid 'glass' is transformed to a liquid-like 'rubber' (Y. Roos, 1995). Crystal melting peaks, a first-order phase transition, is observed as an endothermic heat flux associated with the enthalpy change as heat is removed from the environment (Chen, 2013).

The advantages of studying crystallization in the DSC are the small sample required and high sensitivity, but because of the sample size is so small the results from DSC studies are difficult to interpret directly in terms of process operating conditions (Hartel, 2001). Another disadvantage of DSC is when analyzing a sample with higher moisture or a sample made of sucrose and lactose. Sugar dissolves as the temperature increases in high moisture systems, causing a smaller peak to show the heat of solution. Crystalline sucrose has an endothermic transition in the 170 °C to 190 °C region whereas crystalline lactose and sucrose have a complex melting peak in the range of 150 °C to 200 °C causing the peaks difficult to separate. (Hartel, 2001; Nowakowski & Hartel, 2002).

In other research, by using the DSC to measure relatively pure low molecular weight materials such as sucrose, apparent melting would occur. Apparent melting research shows the differences that occur with changing in heating rates and weights in DSC measurement (Lee, Thomas, & Schmidt, 2011a). The limitations of the DSC analytical tool stems from the structure of the apparatus. The furnace heats the sample while the thermocouple is at a higher temperature

because it is not in direct contact with the sample. This gap between the sample and thermocouple introduces thermal lags which can change the melting temperature (Lee, Thomas, & Schmidt, 2011a). Several sucrose attributes, mentioned in section 1.2. show variation in DSC results which can alter the measurement of sucrose crystallinity.

### **1.4.3. Microscopy**

Microscopy has been a historical foundation for studying food structures, including crystals (Hartel, 2001; Kaláb et al., 1995). Many microscopy techniques for measurement include; conventional, polarized light, scanning electron microscope (SEM), transmission electron microscopy (TEM), confocal scanning laser microscopy (CSLM), and atomic force microscopy (AFM). Microscopy provides useful qualitative information of crystalline structure, and can also give quantitative information from well-prepared samples. Microscopy is an extension of visual examination of foods, and the different steps in preparation (i.e. grain milling or protein denaturation) of the food sample can change the visualization food structure from its original state (Kaláb et al., 1995).

Microscopy techniques such as SEM and CSLM have different sample preparations. For example, in CSLM, fluorescent dyes are chosen depending on the structural element of interest that needs to be illuminated within the food (Hartel, 2001). The dye will interact with structural elements and may act as an impurity and alter crystallization. Depending on the analysis, sample, and/or matrix of food, all these factor into determining which dye to be used in analysis, and the application method (i.e. surface application, within manufacturing a product, and etc.). SEM sample preparation, in order to keep crystalline structures intact, involve freezing and drying since water from the sample can attenuate the electron beam and reduce visibility. Gold or platinum coating is needed to provide a conducting surface. This sample preparation and other SEM

types allows for a qualitative and quantitative image analysis without dilution or dispersion (Hartel, 2001).

#### **1.4.4. X-Ray Diffraction**

An optical technique such as small-angle X-ray diffraction (XRD) is used to study surface structure and crystal/phase orientation (Merrifield et al. 2011). Different crystal sizes can be evaluated using XRD, from nanometers to several millimeters. A beam of light is passed through a dispersed sample and the light beam is measured and correlated to different crystal characteristics such as size, number, and shape (Hartel, 2001). Different XRD patterns represent the short-spacing in crystal lattices (Grotenhuis, 1999). XRD is appropriate to study polymorphic phases because of the characteristic pattern in the range of 3.0 – 6.0 Å. It can also reveal details of crystallization, melting, and phase transition processes as a function of time and temperature. The XRD total diffracted intensity can quantify the crystalline material in the sample (Malssen, 1996).

Two different ways to determine sucrose crystallinity from the diffraction pattern include the total area under the characteristic sucrose peak and from height of the peak (Chinachoti & Steinberg, 1986). Depending on other ingredients in the matrix or mixture, interference can occur and effect the correlation. Ingredients such as starch and fat can exist in crystalline form, and even though it can have other characteristic peaks outside of the area of sucrose, it can have an effect on the sucrose crystallinity measurement. Chinachoti's research showed that sucrose crystallinity (calculated vs. measured through XRD) had a high correlation under specific sample preparations and crystalline sucrose growth methodologies. Interferences from other crystalline food can pose quantification issues showing a higher than expected values of crystalline sucrose because other ingredients would be additive to the total amount.

According to Seyer and others, the drawback to using this method is that the limit of detection for the XRD technique is around 5 to 10%, and sometimes requires

further particle size reduction (Seyer et al., 2000). This is a disadvantage of this method since sample manipulation adds time and complexity to sample preparation and possible inline technology.

#### **1.4.5. Nuclear Magnetic Resonance Spectroscopy**

Nuclear Magnetic Resonance spectroscopy (NMR) is a tool used for the investigation of complex mixtures for chemical compound identification and structural characterization. NMR requires minimal processing procedures and a minimal sample amount (Cosonni, 2011). It is an essential analytical tool to interpret structural information of unknown natural and synthetic compounds. The advantage of NMR is providing simultaneous access to both quantitative and qualitative information (Simmler, 2014). In a nondestructive and nontargeted manner, NMR provides a wealth of information and is widely used in food chemistry to obtain metabolite profiles of different kinds of biofluids and foods (Wei, 2014). Solid-state NMR (ssNMR) can go through phase transitions because high spinning speeds are required to collect a high resolution therefore this technique would not be ideal for quantification of crystallinity (Stephenson et al., 2001).

There are several things to consider when building a quantification method with NMR techniques or more specifically, ssNMR. Inaccurate spectral intensities can occur when relaxation properties are not factored into the assay development along with variance which can stem from a heterogeneous sample mixture in the preparation step (Bugay, 2001). NMR measures the crystallization of sucrose in by observing the interaction between sugar and water molecules and the relaxation rates of water molecules in a sugar solution (R W Hartel & Shastry, 1991). This enables the use of NMR to understand structure and crystallization of sucrose, but this is on a bulk sample and does not facilitate for further development in inline technologies. The limitation of using NMR is not only the

sample preparation difficulties, but also the high cost in comparison the IR spectroscopy (Bugay, 2001).

#### **1.4.5. Infrared Spectroscopy**

Compared to high performance liquid chromatography (HPLC), ultraviolet (UV)-visible spectrophotometry, capillary electrophoresis, gas chromatography/mass spectrometry, and electrochemical methods vibrational spectroscopy provides fundamental information about the chemical content. Along with fundamental information, vibrational spectroscopy (Raman and Infrared) can measure multiple analytes simultaneously and non-invasively (Shih, 2011).

#### **1.4.6. Raman Spectroscopy**

Raman spectroscopy is a section of vibrational spectroscopy where a sample is exposed to an intense laser. A Raman-active spectrum of vibrational modes which are induced from the sample molecules shows molecular structure information through the measurement of molecular vibrational state energy transitions (Paradkar, 2006).

Raman spectroscopy has an advantage of analysis of aqueous samples because little scatter is produced in the 0-3000  $\text{cm}^{-1}$  region from water (Zhang et al., 2005, Delfino, 2010). More recently optical methods such as Raman and infrared spectroscopy are becoming more important in food production and quality control (Chao et al., 2008). Raman spectroscopy has allowed for the characterization of many different food systems including the ability to discriminate amount different kinds of sugars (Delfino, 2010). Raman has been a complementation to infrared spectroscopy (IR), where peaks which would show in Raman spectroscopy would not appear in IR spectra.

Using Raman mapping on a complex sample, spatial distribution and sizes of constituents can show a wealth of information. This information enables the understanding of a 2D surface of a food product; this can show spatial



differences that occur through formulation variances or processing changes. Food product surfaces are not all created equally, the heterogeneous nature of food product surfaces can change the organoleptic and storage quality. By studying the 2D structure of a food product surface, food manufacturers can fine tune a product to meet those different properties. Raman spectroscopy has been used in the food industry historically to investigate individual points and individual ingredients within chocolate, but not final chocolate products (Lamour, 2010).

The source power is a disadvantage of this technique, because the laser which emits a monochromatic radiation in the 400 – 780 nm range. Molecules can be excited to energy states that are above the vibrational level, returning as fluorescence which can overwhelm the signal (Reuter, 2013). Another disadvantage is the arrangement of powdered samples such as lactose can change the measurement (Lehto et al., 2006). Particle size have shown to change the Raman peak responses making it difficult to analyze crystal powders with different sizes (Pellow-Jarman et al., 1996). Raman collection efficiency is compromised by the process of confining the light and this disadvantage can be lessened by long accumulation times (Smith & Dent, 2005). Calibration can be challenging because the life of the bulb and temperature can affect the lamp energy. These factors along with correction polynomials must be used to calibrate for quantitative methods (Smith & Dent, 2005).

#### **1.4.7. Near-Infrared Spectroscopy**

Near-infrared (NIRS) and mid-infrared (MIRS) spectroscopy have been used for authenticity studies of foods such as the assessment of vegetable oils, olive oil, honey, and coffee (Paradkar, 2006). The NIR spectroscopic method uses the 800 nm to 2500 nm region in the electromagnetic spectrum. Using NIR as an instrumental method to quantify total dietary fiber content of cereal enables for a quicker analysis, non-destructive sample handling, and safer methods since the

fiber assays produce a considerable amount of chemical waste (Archibald, 2000).

A NIRS quantification technique was found to be effective at quantifying crystallinity in binary powder mixtures, but this was more specific to pharmaceutical use where regions of 1436 and 1474 nm were used in the methodology (Seyer et al., 2000). This method showed to have precise measurements, but was built around low moisture (0.76 to 2.84%) conditions in a non-food matrix which is not ideal for development in food applications. A disadvantage of NIRS is that it is a tool based on intricate calibration procedures which comprises of complex chemometrics and training sample set (McClure, 1994). The advantages of speed, simple sample preparation, real-time measurement of multiple properties from one spectrum, and nondestructive sample handling far outweigh the disadvantages (Reuter, 2013; McClure, 1994). In all forms of spectroscopy, historical spectra can be reevaluated at a later date using new calibration methodology to determine an old or new trait (Bittante and Cecchinato, 2013).

#### **1.4.8. Mid-Infrared Spectroscopy**

Dispersive IR was the precursor spectrometer in the 1940's prior to the FTIR development for advanced research in the 1960's where each wavelength was measured one at a time (Larkin, 2011; Thermo Nicolet Corporation, 2002). The dispersive infrared instrument (Figure 5) passes energy from a source to a sample and reference through a chopper to moderate the energy moving to the detector. The grating separates the different wavelengths and directs individual wavelengths through the slit and then into the detector. One at a time, each wavelength is measured by moving the grating to the select wavelength and the detector measures the energy at each frequency. This process is time consuming if multiple wavelengths are needed for analysis, because the energy

reaching the sample must be limited to measure data points closely spaced together (Nielsen, 2010; Thermo Nicolet Corporation, 2002).

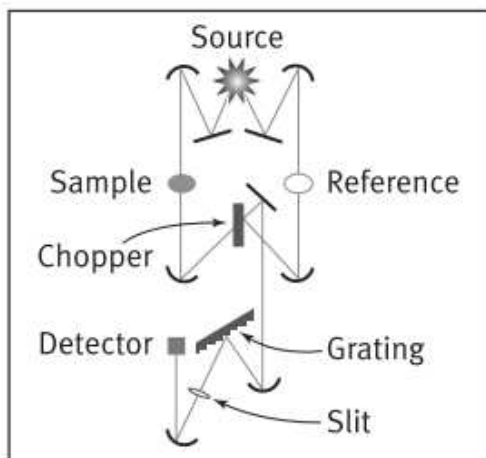


Figure 5: Dispersive spectrometer diagram (Thermo Nicolet Corporation, 2002)

The FTIR instrument uses the interferometer system (Figure 6). The energy goes from the source to the beamsplitter which divides the beam into two where one is transmitted onto a fixed mirror and the other to a moving mirror (Griffiths & Haseth, 2007; Nielsen, 2010; Thermo Nicolet Corporation, 2002). The moving mirror moves back and forth at a constant velocity depending on the laser wavelength and both beams are reflected back into the beamsplitter. The difference in beam distance from the moving versus fixed mirror produces an interferogram goes to the sample where some energy is transmitted and travels to the detector (Griffiths & Haseth, 2007; Nielsen, 2010; Thermo Nicolet Corporation, 2002). Fourier Transform (FT) is a mathematical treatment which allows for the simultaneous collection of wavelengths through the detector (Nielsen, 2010).

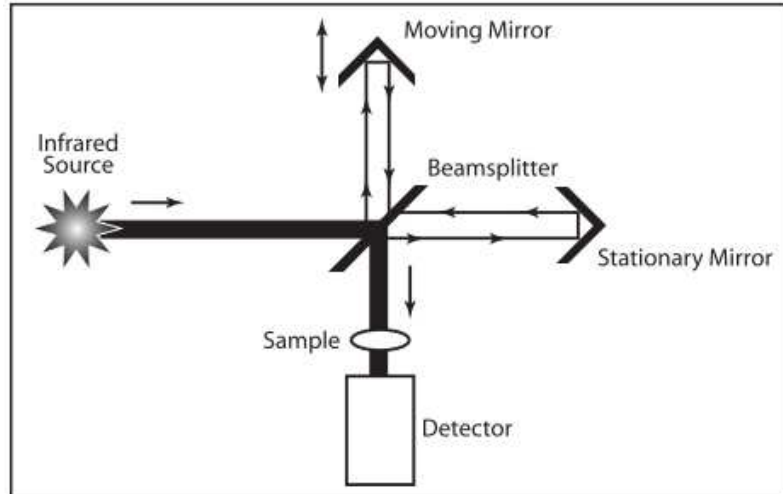


Figure 6: Michelson Interferometer Diagram (Thermo Nicolet Corporation, 2002)

FTIR technology produces a fingerprint which is unique to each molecular structure with increased speed from the simultaneous measurement collecting a scan every second (Thermo Nicolet Corporation, 2001; R. H. Wilson, 1990). Lower cost and improvement in the performance of instrumentation has driven an increase in interest in food applications enabling rapid analysis and inline control (Wilson, 1999). In addition to the multiplex advantage of simultaneously collecting data at all different wavelengths, throughput and precision are also advantages of using FTIR instead of dispersive IR (Thermo Nicolet Corporation, 2002; R. H. Wilson, 1990).

FTIR has been widely used as a secondary method, requiring calibration, for predicting and quantifying chemical properties of different materials. Even though more research is essential in FTIR in food applications, there has been research regarding the use of MIRS to quantitatively determine main components of food (Bittante and Cecchinato, 2013). Nondestructive and rapid infrared spectroscopy methods are advantageous to determine qualitative attributes of different products such as milk powders without the laborious chemistry analyses in laboratories (Wu, 2007). In cases such as analysis for fat content in milk powders, several other methods are available such as Soxhlet extraction,

Babcock, and Gerber methods. These methods require handling of hazardous chemicals and require sample destruction.

Adulteration and component analysis has traditionally been the main use for food analysis using FTIR (Kelly & Downey, 2005). Library searches and subtraction spectra allow for the spectroscopist to search for spectra attributes for compounds specific to an ingredient or a foreign, unknown material. Known substances within a library allow for identification and qualification purposes, however quantification of those substances require further method development. Furthermore, in the case of sucrose, it would be simple to build a method to quantify or identify for sucrose within a sample, but the challenge exists more in specificity of quantifying crystalline sucrose.

The fingerprint region, a narrative region of MIRS, is used to identify particular molecular vibrations. This area can depict certain vibrations within sucrose as a molecular structure. To quantify sucrose crystallinity, however, further examination of the data is required of the entire spectral regions including the fingerprint region. The study of the data includes determining and classifying peaks which correlate in relation to the concentration of sucrose crystallinity, instead of just the sucrose molecule. Since the FTIR measures for bond vibrations of the molecular structure, sucrose, whether amorphous or crystalline, has the same molecular structure but different physical structure. The key to this research is to determine which peaks in the spectral images containing crystalline sucrose represent the physical changes in the macro structure of sucrose versus the molecular or micro structure. This is where the training of the FTIR from a primary method such as DSC is necessary.

Ottenhof, Macnaughtan, and Farhat (2003) determined that the MIRS region which was dominated by C-O and C-C stretching vibration could be used to monitor changes in the physical state of sugar. Not only does it allow for the analysis of the physical state of sugar, but it also enables the study of chemical

identity of mixed systems (Ottenhof et al., 2003). The research of using FTIR to measure for sucrose crystallinity is a challenge in many aspects. In addition to the mentioned complexities, high moisture samples can have responses which fill up spectra causing the O-H region ( $\sim 3200\text{ cm}^{-1}$ ) to dominate and overcome the spectral with incoherent peaks. The build of the methodology using FTIR to quantify for sucrose crystallinity requires the method to choose peaks which are independent of moisture.

#### **1.4.9. FTIR Microscopy**

A 2D spatial analysis and quantification would allow for the understanding of surfaces and the map of where attributes exist. A FTIR microscope uses a combination of microscopy and spectroscopy technology to take images of a surface and analyze different points on the surface to create an area map of different constituents. Previous uses for this equipment has been implemented in analyzing old master paintings for pigment origination and counterfeit paintings (Pilc & White, 1995).

The overall advantages of this research enable the technology to quantify for sucrose crystallinity and also create the foundation necessary to understand sucrose crystallinity on a more robust scale which is realistic for the food industry. Furthermore, this lower cost equipment has room to grow in technology which facilitates inline plant technology, spatial (2D) quantification, and low sucrose crystallinity concentration measurement.

## **1.5. Conclusion**

There are several techniques that are available to quantify for sucrose and others which are in the midst of fine tuning the techniques to deliver precise measurements for sucrose. Although this is elevated interest in complex analysis is substantial improvement towards attaining more information faster in most product applications, further development in analysis will enable the solutions for complex systems such as food matrices. Sucrose crystallinity is one piece of a greater picture; it is an attribute that plays a role in texture, organoleptic properties, and storage stability. The elucidation of sucrose crystallinity concentration by the research of the robust, basic methodology for analysis using a rapid yet informational technique such as FTIR allows for a growth in realm. Hybridizing spectral systems is the wave of the future, where development around analysis of products outside of food is enabled by computers with rapid processors and higher memory and complexities in mathematical treatments.

## 2. Materials and Methods

### 2.1. FTIR and DSC Settings

Smart Reflectance Accessory Sample Cup on the Thermo Nicolet 670 FTIR Spectroscopy (Waltham, Massachusetts) bench was used for sample analysis and the build of the calibration curve (Figure 7). The parameters for the bench were run at 128 scans and a nitrogen flush was used to eliminate noise and environmental factors. The background spectrum was taken on a gold mirror prior to the experiment.



Figure 7: Smart Diffuse Reflectance Accessory with Sample Cup Example

The Diamond DSC (Perkin-Elmer, Waltham, Massachusetts) was used to analyze for sucrose crystallinity as a foundation for the FTIR calibration. Samples were held at 0°C for 2 minutes and heated up from 0°C to 200°C at 10°C per minute. DSC was a primary, direct measurement to quantify for sucrose crystallinity. Since the FTIR, a secondary measurement, needed to be calibrated using a primary measurement to build a quantification method, the DSC was the current method chosen for this purpose. The error in measurement using the DSC was  $\pm 10\%$ , therefore the FTIR possessed the same error in measurement since the quantification was built using the DSC parameters.



## 2.2. Methods for Sample Preparation

### 2.2.1. Sample Preparation Using Nujol as a Medium

Analytical grade sucrose, purity (99.9%) (Sigma, St. Louis, MO) was mixed with Nujol (Sigma, St. Louis, MO) initially to measure for sucrose crystallinity concentration. Mineral oil or Nujol was chosen because Nujol is IR inactive, where most of the bands for Nujol are not in areas of interest for most samples (Figure 8).

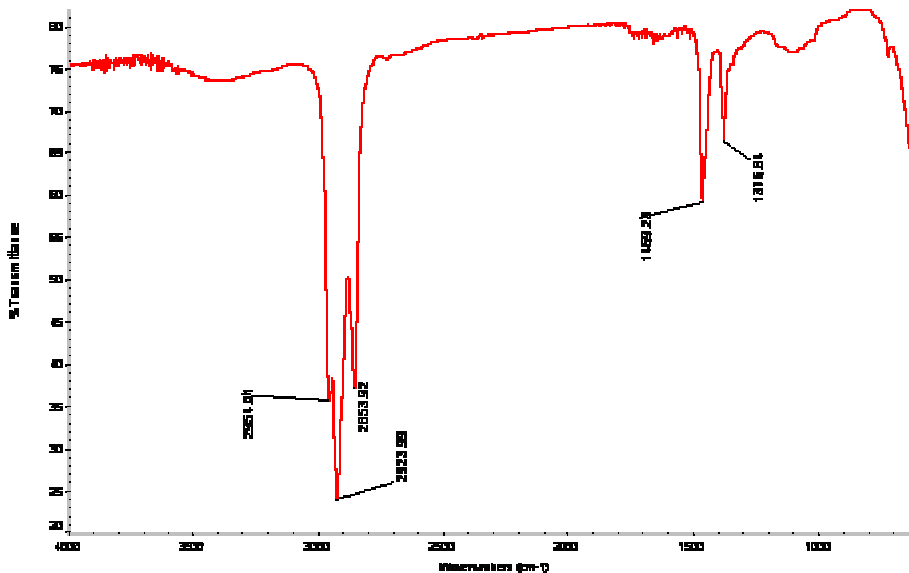


Figure 8: Nujol FTIR spectrum (Linstrom & Mallard, 2013)

Sucrose and Nujol (Table 1) were directly weighed onto a sample tray used for the Smart Reflectance Accessory on the Thermo Nicolet 670 FTIR Spectroscopy bench.

Table 1: Composition of sucrose and Nujol mixtures used in the first FTIR experiment to determine if Nujol would be the proper medium to build a quantification method.

Variation <sup>1</sup>	Sucrose (mg)	Nujol (μL)	Total Weight (mg)	[Sucrose] (%)
1, 2, 3	29.15	24.5	50.10	58.2
4, 5, 6	7.42	92.8	91.17	8.1
7, 8, 9	24.62	-	24.62	100.0
10, 11, 12	-	29.4	29.40	0.0

<sup>1</sup> Variations were run in triplicate on the FTIR

### 2.2.2. Sample Preparation Using 63DE Corn Syrup as a Medium

63DE Corn syrup (Cargill, Minneapolis, MN) was used as another medium to measure for sucrose crystallinity concentration. This was chosen as a medium because it suspended sucrose crystals in a mixture because of the higher viscosity of the syrup. Since the 63DE corn syrup has 17.4 – 18.6% moisture, mixtures were normalized for 18% moisture (see Table 2). Mixtures were prepared in a 4 oz. polyethylene terephthalate (PETE) cup with lid and stirred for 1 minute. All mixtures were prepared and immediately analyzed using DSC and FTIR.

Table 2: Composition of sucrose and 63DE corn syrup mixtures analyzed using FTIR to determine if 63DE was appropriate to use as a method medium

Variation	Sucrose (g)	63DE (g)	Water (g)
1	74.98	25.01	16.48
2	75.00	25.02	16.49
3	24.98	75.02	5.50
4	25.04	75.03	5.50

Spectra were interpreted to determine the change in peak characteristics between 25% sucrose and 75% 63DE versus spectra at 75% sucrose and 25% 63DE corn syrup.

### 2.2.3. Sample Preparation Using 10DE Maltodextrin as a Medium

A low moisture medium, 10DE maltodextrin (approximately 7.6% moisture) was chosen to see how it worked in the FTIR analysis. Maltodextrin, a polysaccharide, is used as a food additive in different processed foods. 10DE maltodextrin did not introduce extrinsic factors upon sucrose such as moisture, it was mixed into a homogenous mixture with sucrose, and because of its dry powdery texture the mixture did not change over time.

Table 3: Composition of 10DE maltodextrin and sucrose mixtures evaluated using DSC and FTIR.

Variation <sup>1</sup>	Sucrose (g)	10DE Maltodextrin (g)	[Sucrose]%	[10DE]%
1	10.03	10.03	50	50
2	7.50	2.50	75	25
3	2.50	7.50	25	75
4	10.00	0.00	100	0
5	0.00	10.00	0	100
6	1.00	9.00	10	90
7	9.00	1.00	90	10

<sup>1</sup> Variations were run in duplicate on the FTIR. Mixtures were stirred in 4 oz. PETE cups with lids for 1 minute. Samples were loaded onto the FTIR sample cup in excess and then leveled off to achieve a flat surface. Each variation was run in duplicate and the average spectrum was used to determine peaks to be used in calibration.

## 2.3. Methods for Analysis of Spectra

### 2.3.1. Analysis of FTIR Spectrum of 10DE and Sucrose

Spectra were analyzed using peak intensity ratio analysis to determine which peaks changed and by how much in relation to the composition of DSC determined values of sucrose crystallinity. Peaks which exhibited change between concentrations of sucrose were measured in comparison to peaks which did not change among concentrations (Equation 5).

$$\text{Peak Intensity Ratio} = \frac{P_1}{P_0} \quad (\text{Equation 5})$$

Where  $P_1$  = Peak intensity at a certain wavelength that did change

Where  $P_0$  = Peak intensity at a different wavelength which did not change

Furthermore, the peaks were compared against each other to determine which peaks would best represent the change the sample was experiencing. Samples at 100%, 50%, and 0% sucrose were used in this calculation to test high and low concentrations of sucrose and a midpoint (Figure 9, 10, 11, 12).

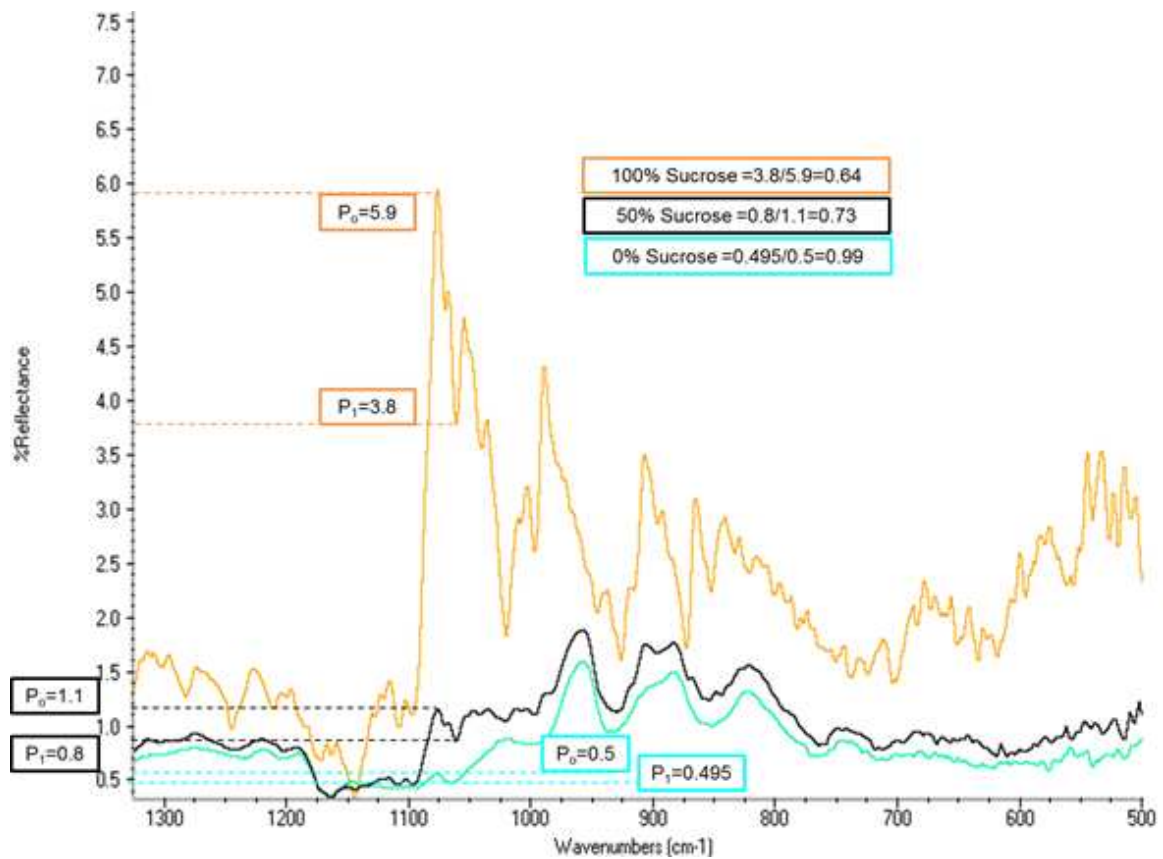


Figure 9: Peak intensity ratio analysis performed around 1090  $\text{cm}^{-1}$  of 100% and 50% sucrose with 10DE maltodextrin and 100% 10DE maltodextrin sample

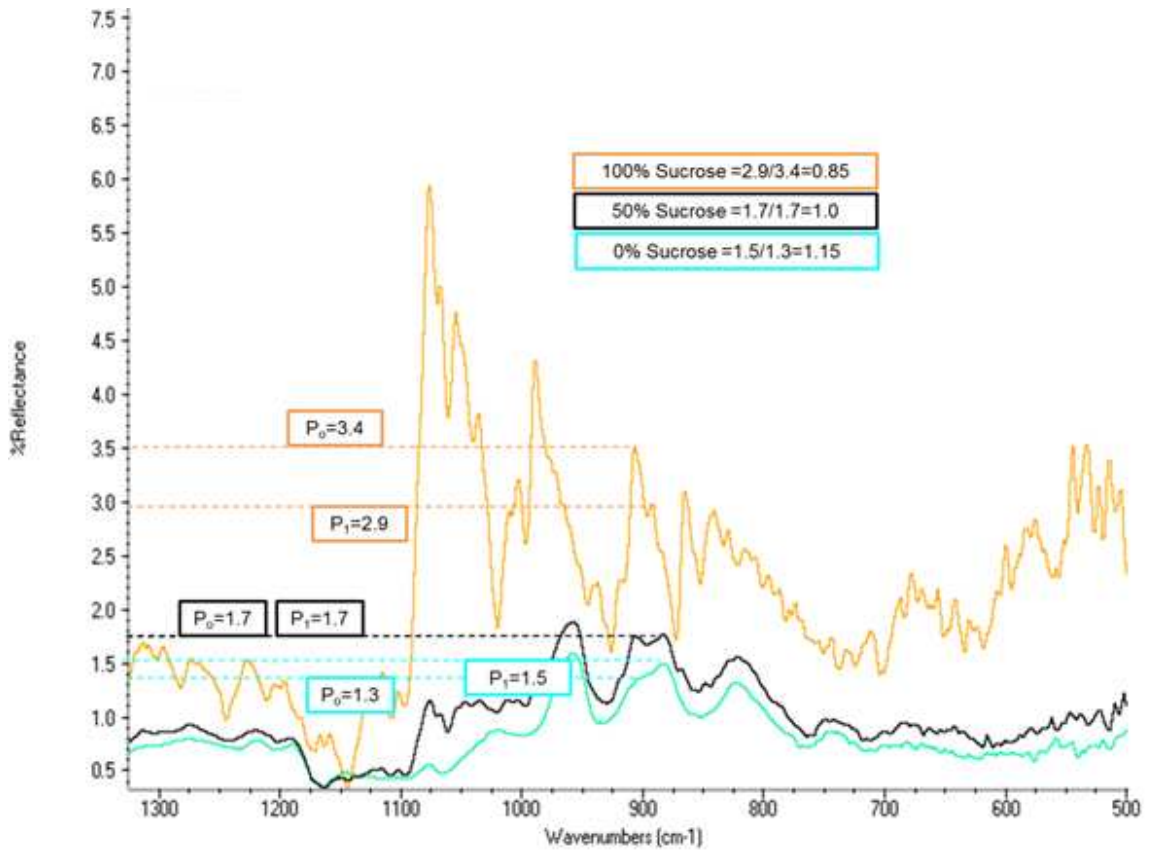


Figure 10: Peak intensity ratio analysis performed around  $900\text{ cm}^{-1}$  of 100% and 50% sucrose with 10DE maltodextrin and 100% 10DE maltodextrin sample

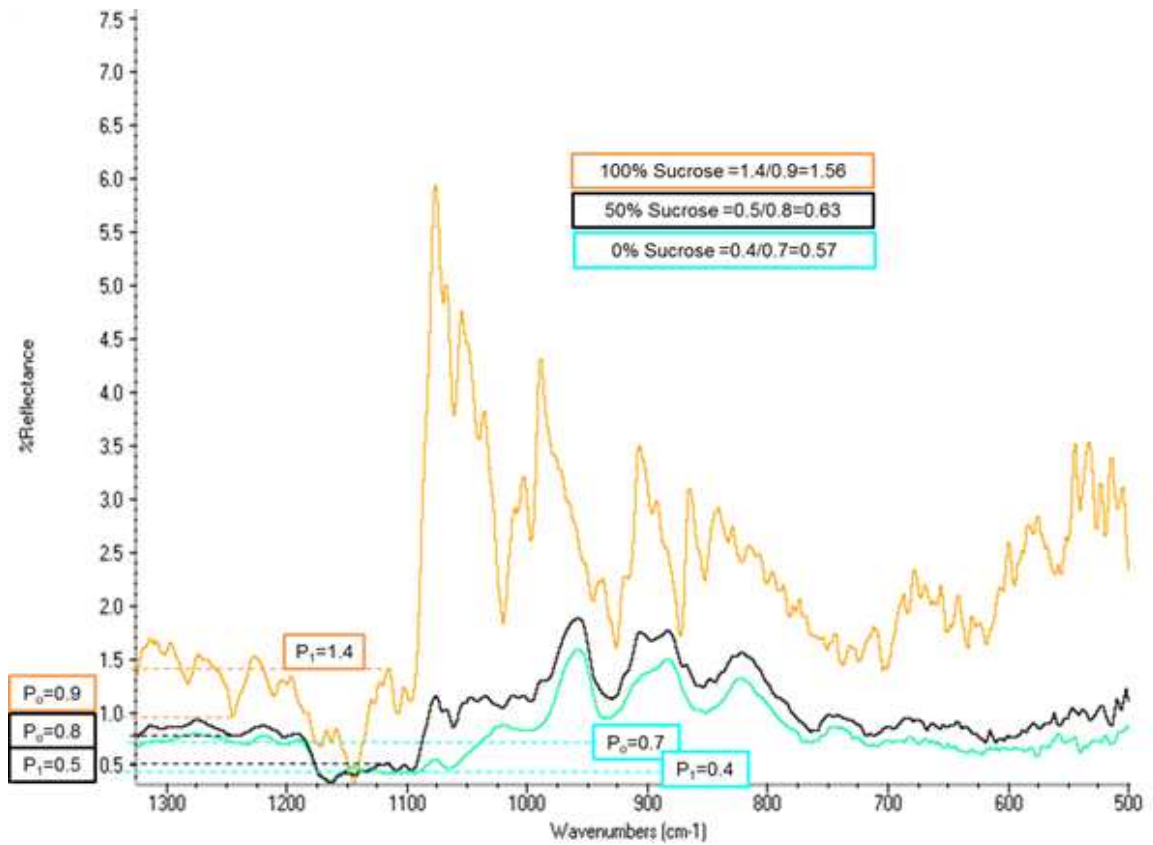


Figure 11: Peak intensity ratio analysis performed around  $1100\text{ cm}^{-1}$  of 100% and 50% sucrose with 10DE maltodextrin and 100% 10DE maltodextrin sample

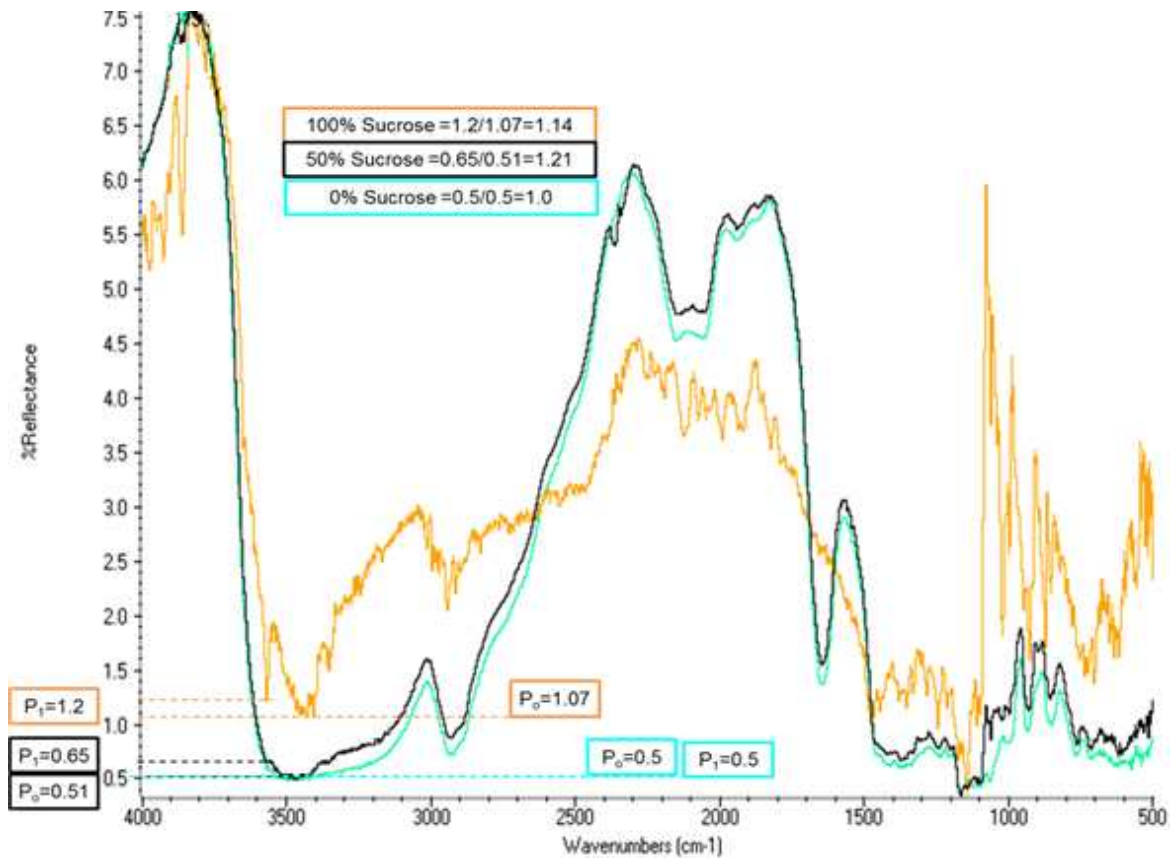


Figure 12: Peak intensity ratio analysis performed around  $3500\text{ cm}^{-1}$  of 100% and 50% sucrose with 10DE maltodextrin and 100% 10DE maltodextrin sample

Values from peaks evaluated using the peak intensity ratio analysis were compared to each other to determine the amount of change different concentrations caused the intensities to shift at each peak (Figure 9,10,11,12).

### 2.3.2. Moisture of 10DE Maltodextrin and the Effects on the Mixture

Moisture can be an extrinsic factor on sucrose crystallinity and also spectra. Further analysis of freeze-dried sucrose and 10DE maltodextrin concentrations was analyzed using FTIR to see if the peaks chosen based on the method in section 2.3.1. were affected by moisture in the sample. In addition, peaks from the freeze drying experiment did not shift in intensity between regular and dried samples and therefore were chosen as additional peaks which showed potential.

All variations were freeze dried were prepared using Millrock Technology LD53S3 (Kingston, NY) freeze dryer. FTIR were run on all samples to retrieve spectra which represent moisture-normalized samples. Peaks chosen in section 2.3.1 were analyzed again to determine if the peaks shifted in intensity compared to when the samples contained moisture (Figure 13, 14, 15, 16) where darker regions were determined from initial analysis and lighter regions were determined as additional contenders. This was used as a means to confirm the peaks chosen correlated to the concentration of sucrose crystallinity instead of with moisture in the sample analyzed.

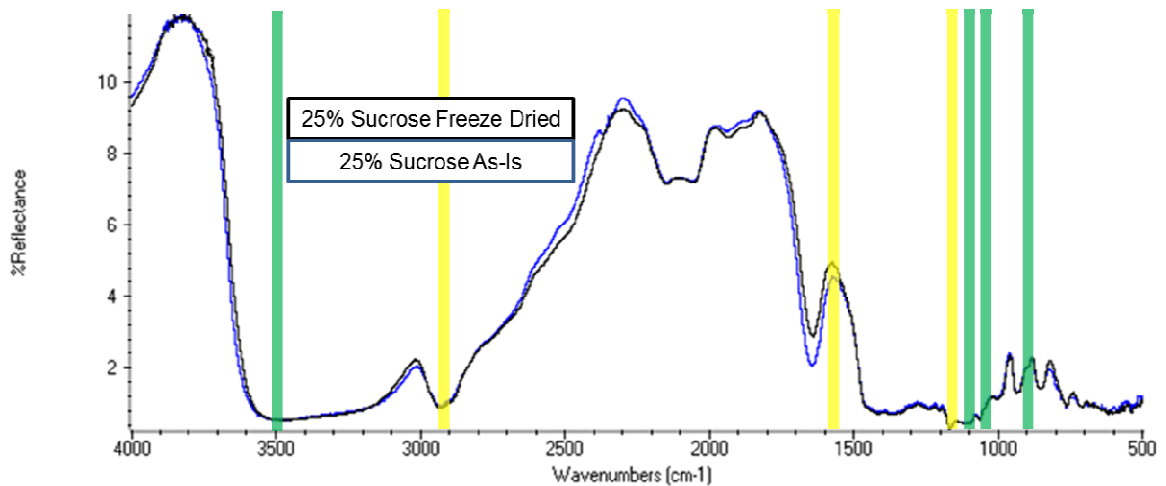


Figure 13: Sucrose at 25% concentration with maltodextrin was evaluated using FTIR bulk method on both the freeze dried sample and sample at 6.0% moisture.



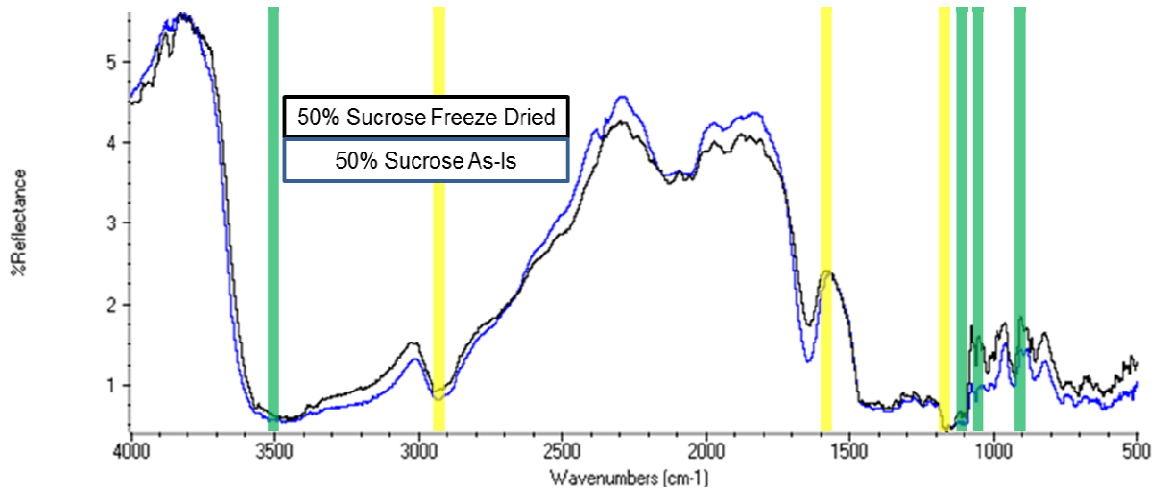


Figure 14: Sucrose at 50% concentration with maltodextrin was evaluated using FTIR bulk method on both the freeze dried sample and sample at 3.6% moisture.

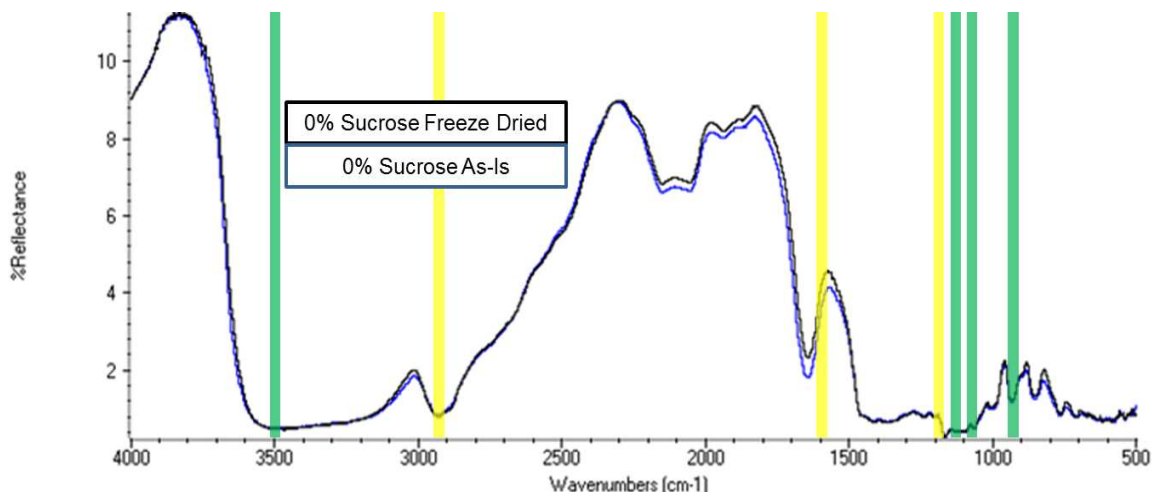


Figure 15: Sucrose at 0% concentration with maltodextrin was evaluated using FTIR bulk method on both the freeze dried sample and sample at 7.6% moisture.

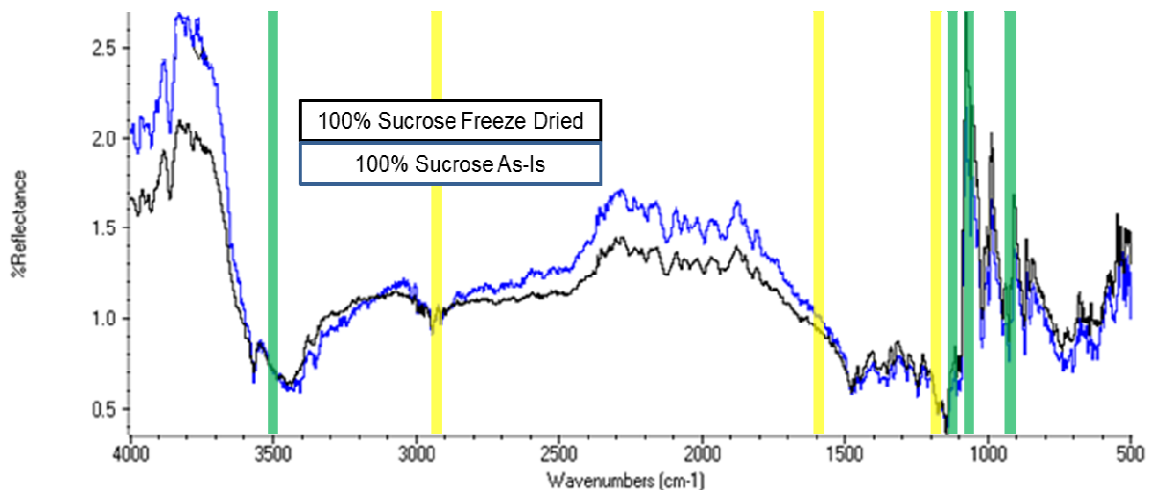


Figure 16: Sucrose at 100% concentration was evaluated using FTIR bulk method on both the freeze dried sample and sample at 0.16% moisture.

### 2.3.3. Evaluation of Peaks from Experiment 2.3.2.

In addition to the peaks from section 2.3.1, the experiment 2.3.2 added additional peaks ( $2925\text{ cm}^{-1}$ ,  $1575\text{ cm}^{-1}$ ,  $1175\text{ cm}^{-1}$ ) to be evaluated because of the low shift in intensity between samples at 7.6-0.16% moisture and the freeze dried samples (Figure 17, 18, 19). These peaks were evaluated using the peak intensity ratio analysis to determine the amount of change each peak had in intensity compared to the concentration of crystalline sucrose.

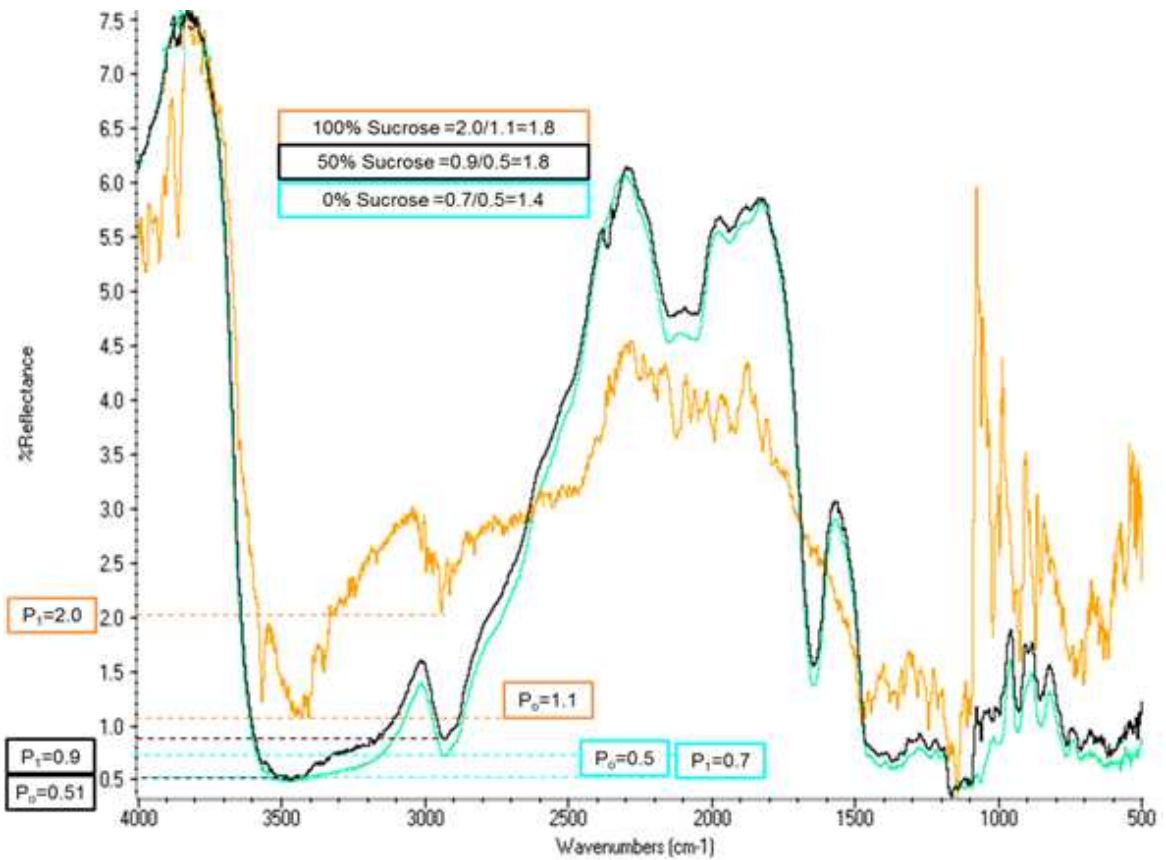


Figure 17: Peak intensity ratio analysis performed around  $2925\text{ cm}^{-1}$  of 100% and 50% sucrose with 10DE maltodextrin and 100% 10DE maltodextrin sample. Peak analysis was determined by experiment 2.3.2.

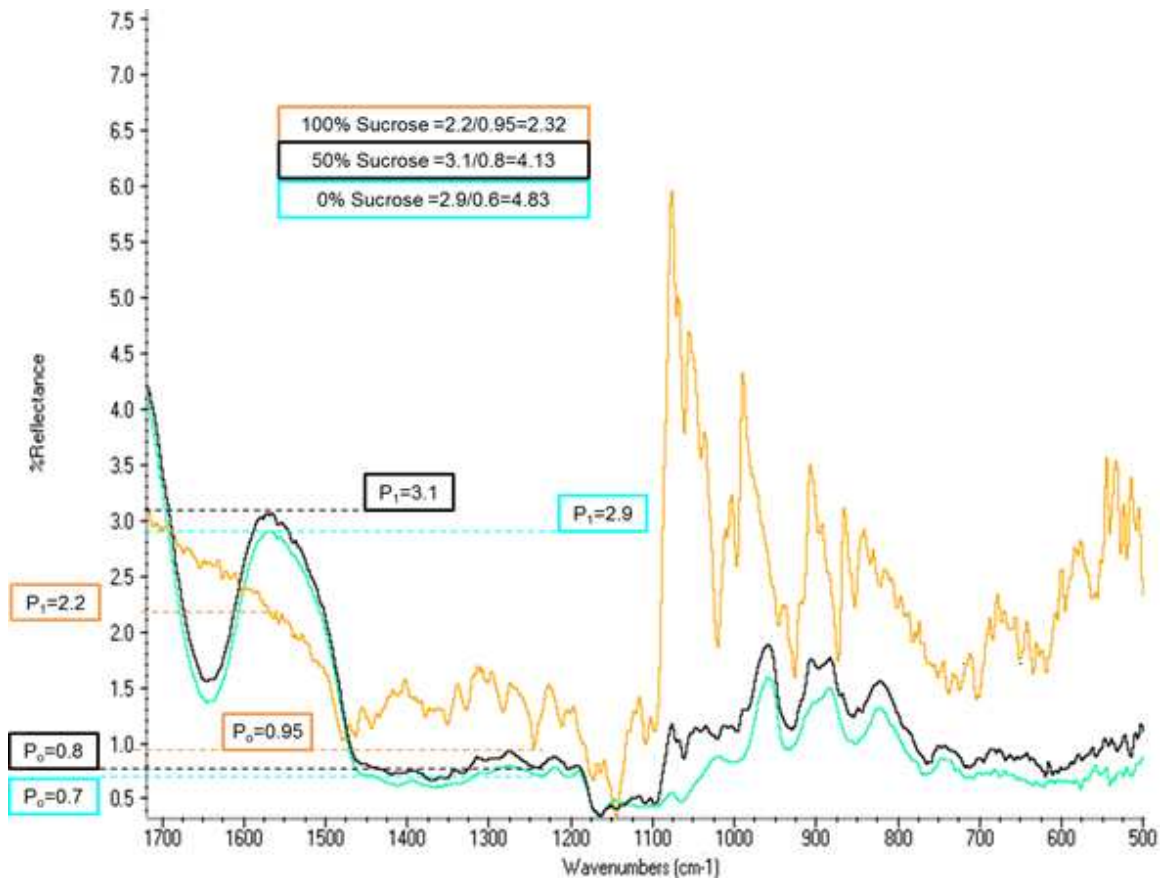


Figure 18: Peak intensity ratio analysis performed around  $1575\text{ cm}^{-1}$  of 100% and 50% sucrose with 10DE maltodextrin and 100% 10DE maltodextrin sample. Peak analysis was determined by experiment 2.3.2.

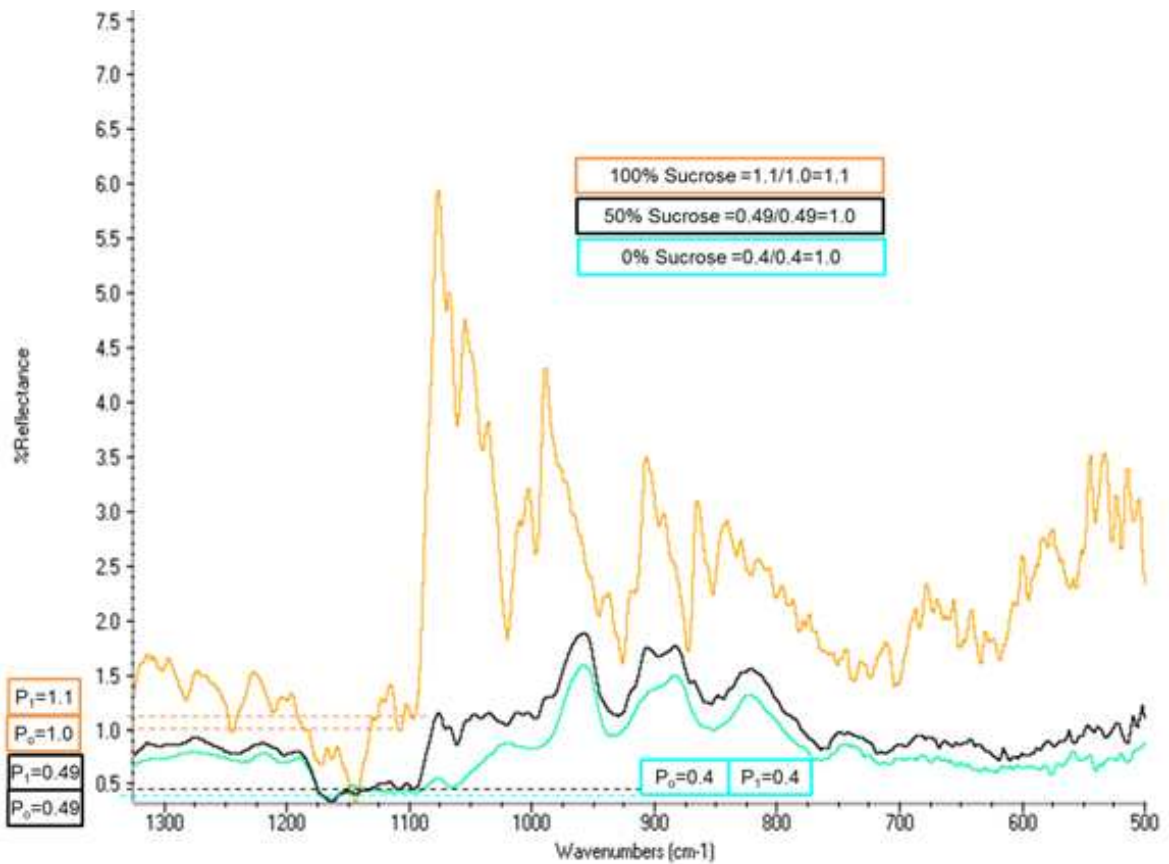


Figure 19: Peak intensity ratio analysis performed around  $1175\text{ cm}^{-1}$  of 100% and 50% sucrose with 10DE maltodextrin and 100% 10DE maltodextrin sample. Peak analysis was determined by experiment 2.3.2.

The interpretation of all the peaks (Table 4) was determined by the previous experiments based on general spectral interpretation literature (Griffiths & Haseth, 2007; Socrates, 2001).

Table 4: Regions of FTIR spectra evaluated using the peak intensity ratio analysis at different levels of sucrose with corresponding FTIR interpretation.

Regions	FTIR Interpretation
3500 cm <sup>-1</sup>	OH/Phenol Stretch
1100 cm <sup>-1</sup>	Tert-OH or Phenols
900 cm <sup>-1</sup>	Mono sub alkenes C-H bond
1090 cm <sup>-1</sup>	Secondary Alcohols
1575 cm <sup>-1</sup>	Aromatic C=C or Carboxylates
2925 cm <sup>-1</sup>	Methyl
1175 cm <sup>-1</sup>	Esters

Table 5: Regions of FTIR spectra evaluated using the peak intensity ratio analysis at different levels of sucrose.

Regions	Concentration (%) of Sucrose to Maltodextrin (10DE)		
	100	50	0
3500 cm <sup>-1</sup>	1.14 <sup>a</sup>	1.27	1.00
1100 cm <sup>-1</sup>	1.56	0.63	0.57
900 cm <sup>-1</sup>	0.83	1.00	1.15
1090 cm <sup>-1</sup>	0.64	0.73	0.99
1575 cm <sup>-1</sup>	2.32	4.13	4.83
2925 cm <sup>-1</sup>	1.82	1.80	1.40
1175 cm <sup>-1</sup>	1.10	1.02	1.00

<sup>a</sup>Ratio values are unitless

## 2.4. Calibration Curve Methods

### 2.4.1. Calibration Curve Experiment to Determine Peak(s) of Interest

Regions determined by section 2.7 along with other peaks found through resources which characterized the vibrational spectra of sucrose (Brizuela et al., 2012) were individually used in different statistical calibration tools (i.e. Beer's Law, Partial Least Squares, and Classical Least Squares). TQ Analyst® (Thermo Nicolet, Waltham, Massachusetts) was used to process the spectral data and correlate it to the concentration determined using DSC. A Performance Index (PI)

in TQ Analyst® indicated how well the calibrated method could classify the validation standards (Hashim et al., 2010). The higher the PI value the closer the standard was to its class. The algorithm to determine the PI was based on the root mean square error of prediction (RMSEP) (Equation 6).

$$RMSEP = \sqrt{\frac{1}{N} \sum (\hat{y}_{i,pre} - y_{i,ref})^2} \quad (\text{Equation 6})$$

Where  $N$  is the number or size of the test set, and  $\hat{y}_{i,pre}$  and  $y_{i,ref}$  are the prediction and reference value of the sample (Beebe et al., 1998; Mark & Workman, 2010). The performance index gives a score based on the RMSEP response. The lower the RMSEP the better the performance because it is essentially the average distance between the predicted and actual values, and the closer the PI is to 100.

All of the statistical calculations were automatically calculated in TQ Analyst®. The SEE was the measure of the accuracy of the validation set of spectra in a regression and SEP was the measure of the accuracy of the calibration spectra in the regression. The ratio of these two values would calculate the consistency or robustness of the quantification method. The bias was the amount of difference between the averaged calibration values and the averaged predicted values (Archibald & Kays, 2000). The closer the correlation coefficient was closer to +/-1 the easier it was for one variable to predict another (Brereton, 2007). The number of factors does not indicate that “more is better”, instead the proper amount of factors is the balance between introducing enough spectra to lower prediction error and introducing more noise.

All standard spectra were used as calibration spectra at the different regions of interest from Table 3; 14 spectra total. The correlations that show a PI greater than 60 would advance into the data culling portion of the data analysis. The TQ Analyst® tool was used to cull spectra from the calibration group of spectra to be

either used as validation spectra or to ignore completely. This allowed confining the calibration curve to show a better performance index.

#### 2.4.2. Partial Least Squared Method Development

All three peaks  $1087\text{ cm}^{-1}$ ,  $991\text{ cm}^{-1}$ , and  $909\text{ cm}^{-1}$  were determined by section 2.8. to move forward with in a PLS quantification method by the PI values. All spectra used previously for calibration were used in this method and data was culled or determined as validation spectra by fine tuning the method.

Table 6: Different PLS combinations performed to determine which was most effective at quantifying sucrose crystallinity.

Regions	$909\text{ cm}^{-1}$	$991\text{ cm}^{-1}$	$1087\text{ cm}^{-1}$
$909\text{ cm}^{-1}$		x	x
$991\text{ cm}^{-1}$			x
$1087\text{ cm}^{-1}$			

#### 2.5. Applications of Sucrose Crystallinity Quantification Method in Food Products

Samples of branded commercially available mixes included a sugar cookie, white cake, and chocolate cake mixes were analyzed using DSC and FTIR bulk measurement. The percent sucrose crystallinity was measured using a DSC method similar to 2.1 and the percent sucrose was determined by a High Performance Liquid Chromatography (HPLC) method used in industry (AOAC Method 997.20). Percent sucrose crystallinity was measured using the FTIR method mentioned in section 2.1.



## **2.6. Methods for FTIR Microscope**

### **2.6.1. FTIR Image Using FTIR Microscope**

Samples with ranging sucrose and 10DE concentrations were used in a FTIR microscope (Nicolet Continuum IR, Waltham, Massachusetts) to explore surface analysis of a bed of sucrose and 10DE mixture. Samples were mixed by shaking in 50 mL centrifuge tubes for 1 minute. An excess amount was scooped and placed in a small vessel with a diameter of 15 mm and a height of 10 mm (Corning 9999-24, Corning, New York). The excess sample was leveled off and was placed on the microscope stage.

The FTIR microscope used the OMNIC programming analogous to the regular FTIR apparatus with the additional Atlas imaging software. A small mosaic comprised of a 5 x 5 squares where each square is 400  $\mu\text{m}$  x 400  $\mu\text{m}$  in size (2000  $\mu\text{m}$  x 2000  $\mu\text{m}$  total area) was taken across a small area on the surface of each of the samples and four points were analyzed with the FTIR scans (200 scans per point). The mapped surface spectra was split into individual spectra and used in the quantification method.

### **2.6.2. Intrinsic Factor - Effect of Crystal Size**

Analytical grade sucrose was ground using a coffee grinder (Mr. Coffee, Cleveland, Ohio) for 1 minute 30 seconds until a powdery consistency was achieved. Rotap (W.S. Tyler, Mentor, Ohio) was used to sieve different fractions of sucrose. Fractions thru sieve No. 80 and on sieve No. 270 were used to represent a small crystal size (powdered). Both the granular, in its current form, and powdered sucrose was measured using a particle size analyzer to determine size distribution of both sets of sucrose.

A mixture of 50% sucrose and 50% 10DE maltodextrin, along with 100% sucrose, and 100% maltodextrin were analyzed using the FTIR microscope. This

was used to determine the effect of particle size on the image. A 250  $\mu\text{m}$  x 250  $\mu\text{m}$  map was taken at 128 scans per point at each corner of the map (Figure 20).

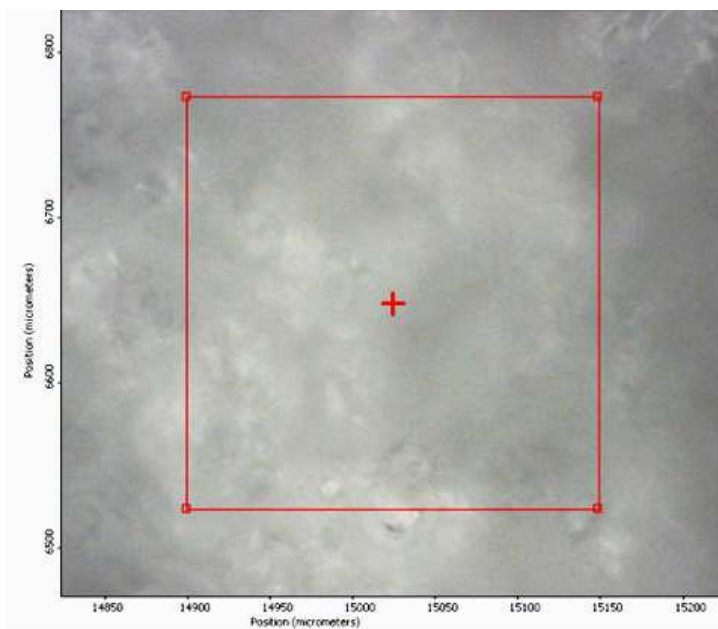


Figure 20: An example window of a mapped surface where scans from the FTIR were taken at each point.

### **3. Results and Discussion**

#### **3.1. Sampling System for FTIR apparatus Determination**

Diffuse reflection Infrared Spectroscopy (DRIFTS) is where a portion of the radiation is reflected off of several particles of a sample before exiting the sample and radiation emerges at random angles from the surface through  $180^\circ$  (Nielsen, 2010). This provided superior performance of the spectra because foods (ingredients, products) created an uneven porous surface. Where intensity couldn't be maximized through other FTIR sampling methods with minimal sample preparation, it could be through DRIFTS because of several incidents of light entering with multiple reflected back into the detector.

The sample cup format was advantageous to this research because the method allowed minimal sample preparation. This form of sample preparation also allows for a multiple beam response, which reduces the noise in the spectra and is also analogous to a larger aperture on the FTIR microscope. Especially with a porous surface or heterogeneous surface, managing diffusely scattered radiation and specular reflected radiation could have been an issue, but the Smart Diffuse Reflectance accessory was highly effective at managing those attributes (Thermo Fisher, 2007).

#### **3.2. Effect of Using Nujol and 63DE for Quantification Method Medium**

Nujol was not used as a medium to build the calibration curve for the quantification method after evaluating the spectra and sample preparation methods. Since the initial build of the calibration curve used a sample cup apparatus on the FTIR the sucrose crystals would sink to the bottom of the cup because of the low viscosity of the medium (Figure 21). This did not allow the FTIR to accurately measure the total concentration of sucrose in Nujol since the surface did not contain the sucrose crystals.

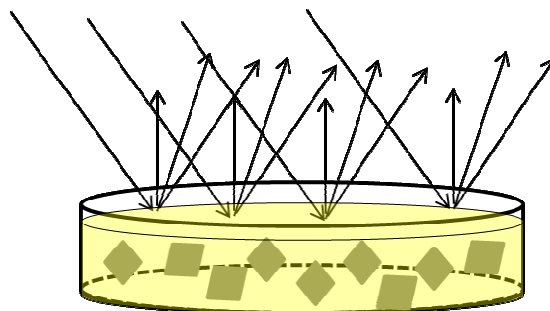


Figure 21: Example of sucrose (squares) and Nujol (shaded area) mixture with incoming incident of light entering and leaving the surface of the Nujol versus the entire sample.

After evaluating the sample preparation and moisture confounding the spectra, corn syrup was not used as a medium. Even though the corn syrup gave a homogenous mixture initially when the sucrose was suspended in the viscous material, over time it would settle out and affected the accuracy of the FTIR spectra. In addition, 63DE corn syrup introduced moisture into the sample, and although this extrinsic factor was representative of realistic food matrices it was important to have a medium that did not affect the sucrose crystals as much as possible for the calibration of the spectra

### **3.3. Sucrose Crystallinity Quantification of 10DE Maltodextrin and Sucrose using DSC**

The DSC analysis was performed on the samples from Table 2.3 and was used to calibrate the quantification method for the FTIR.

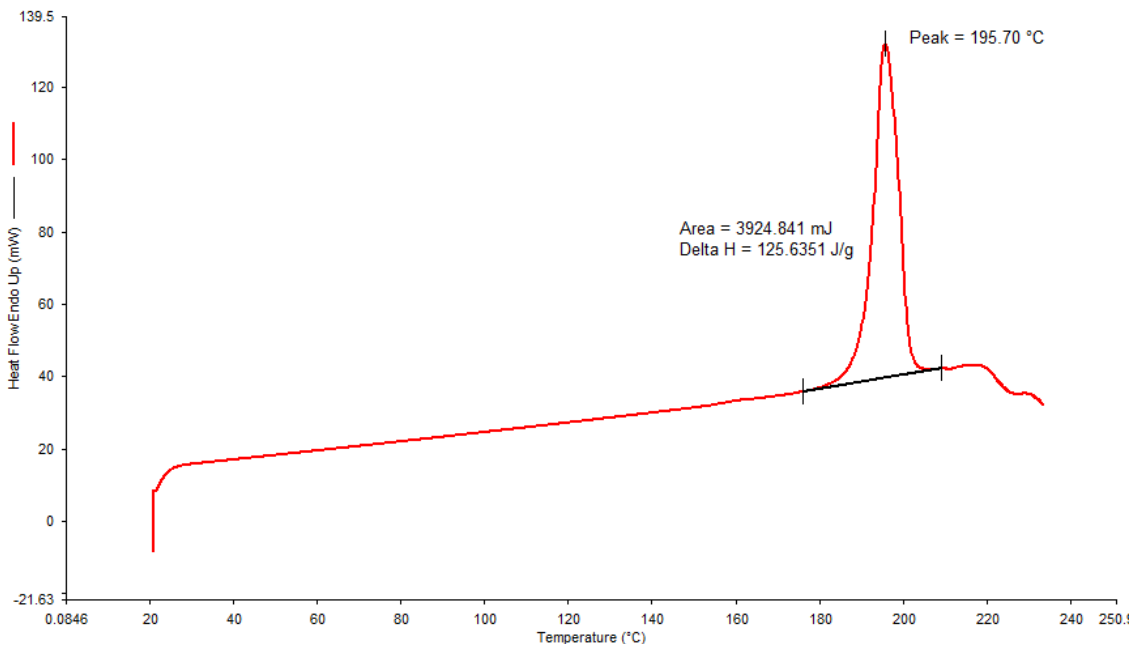


Figure 22: A example DSC thermogram of 100% analytical grade sucrose with a delta H of 125.6 J/g which was used to calculate the concentration of sucrose crystallinity of a bulk sample.

The melting enthalpy of sucrose (135 J/g) was used to calculate the percent crystallinity using Delta H information from the DSC thermogram (Figure 22, Equation 7).

$$\% \text{ Crystallinity} = \frac{\Delta H_{\frac{g}{J}}}{135 \frac{J}{g}} \times 100 \quad (\text{Equation 7})$$

Further normalization for moisture and the amount of crystalline sucrose was performed to correct for the amount of moisture in the sample (Table 7) using the following equations (Equation 8 and Equation 9).

$$\% \text{Crystallinity (moisture corrected)} = \frac{\% \text{Crystallinity of total sample}}{(1 - \text{Moisture of Sample})} \quad (\text{Equation 8})$$

$$\% \text{Crystallinity Normalized} = (\% \text{ sucrose}) \times (\% \text{crystallinity (moisture corrected) at 100\%}) \quad (\text{Equation 9})$$

Table 7: The measurement of percent crystallinity of sucrose mixtures with 10DE maltodextrin determined by DSC

Sucrose in 10DE (%)	Moisture (%)	Average Delta H of Entire Sample (J/g) ± SD <sup>a</sup>	% Crystallinity (total sample) (%) ± SD	% Crystallinity (moisture corrected) (%) ± SD	% Crystallinity normalized based on 93.2% (%) ± SD
25%	5.408%	26.59 ± 0.46	19.7 ± 0.34	20.8 ± 0.36	23.3 ± 0.02
50%	3.605%	56.82 ± 0.26	42.1 ± 0.19	43.7 ± 0.20	46.6 ± 0.05
75%	1.803%	80.14 ± 0.19	59.4 ± 0.14	60.4 ± 0.15	69.9 ± 0.07
100%	0.000%	125.76 ± 0.13	93.2 ± 0.09	93.2 ± 0.09	93.1 ± 0.12

<sup>a</sup>Standard Deviation

The percent crystallinity which was corrected for moisture was used as the  $y_{i,ref}$  values in the calculation for RMSEP (Equation 5).

### 3.4. Bulk method of 10DE Maltodextrin and Sucrose Quantification Method

Previous media had the disadvantage of added moisture as a factor on the quality of the IR spectra. When initially building the quantification method it was important to see non-confounded spectra to determine which peaks would be best to use. 10DE maltodextrin had a low moisture content (7.62%) and was a dry powder. It was easy to disperse the sucrose in the 10DE maltodextrin, and a

homogeneous mixture was achieved using the sample preparation method mentioned.

Regions chosen among the initial evaluation of sucrose and maltodextrin mixtures and the additional regions from the freeze dryer experiment totaled to seven. All 14 spectra were used in the beginning of each statistical model and peak analysis. Spectra used to calibrate the different models were culled using TQ Analyst® software (Table 8). The software's internal algorithm suggests spectra to be removed based on how different the outlier was from the rest of the population ( $2\sigma$ ). Regions were evaluated with calibration and validation spectra using TQ Analyst® and the performance index (Table 9) was recorded to determine which peaks showed efficacy for the quantification method. This step removed confounding spectra that would have been affected by moisture as confirmed by comparing spectra freeze dried samples compared to the original spectra of samples at unchanged moisture content.

Table 8: Number of spectra culled using TQ Analyst® software at each concentration and region to achieve the performance indexes in Table 9.

Region ( $\text{cm}^{-1}$ )	Beer's Law (% Sucrose)							CLS (% Sucrose)						
	0	10	25	50	75	90	100	0	10	25	50	75	90	100
2925	n/a							n/a						
1104	n/a							n/a						
1087	2	1												
991	1	1						1	1				1	
909		1												
850	n/a							n/a						

Table 9: Performance Index determined by TQ Analyst® at regions found using sucrose and maltodextrin mixtures at different concentrations and analyzed using FTIR.

Region (cm <sup>-1</sup> )	Region Characteristics <sup>a</sup>	Performance Index		RMSEP	
		Beer's Law	Classical Least Squares	Beer's Law	CLS
2925	---	-35.2	-79.5	34.6	46.0
1104	□(C32–O39) <sup>b</sup>	-44.6	-44.6	37.0	37.0
1087	□(C24–O23)	91.6	-79.4	2.16	45.0
991	□(C28–O34)	92.5	89.5	1.92	2.69
909	tw CH2 <sup>c</sup>	92.6	-78.1	1.88	44.5
850	tw CH2	31.5	-323	108	108

<sup>a</sup> Brizuela et al., 2012 <sup>b</sup>stretching mode(□) <sup>c</sup>twisting mode(tw)

Regions specific to sucrose that were chosen from the peak intensity ratio analysis and were verified with the regions listed in previous research by Brizuela (Table 9). The shift in region or window values were slightly different from the paper, a specific analysis for sucrose, because manually measuring the values on hard-copy paper can introduce error from image quality of the printed spectra preventing a clear pinpoint of peaks. This verification step was a way to ensure the regions chosen agreed with spectral interpretation.

Beer's law was performed on all peaks and CLS statistical models such as were applied to see if the performance index (PI) or RMSEP values could be improved further. The Beer's law indicated the regions at 1087 cm<sup>-1</sup>, 991 cm<sup>-1</sup>, and 909 cm<sup>-1</sup> had a superior PI. The CLS calculations show that the regions were not collinear which justifies why a regular multiple linear regression was not used. Instead, the aforementioned regions were used in different combinations (Table 10) and it was determined that the three regions together in a PLS quantification method gave the best PI of 96.3 and RMSEP of 0.925. These values were calculated within the computer software which used a combination of Equation 3, 4, and 6 to determine the PI.



Table 10: PI values of different combinations of regions chosen based on PI and RMSEP values of statistical models from Table 8.

Regions	909 $\text{cm}^{-1}$	991 $\text{cm}^{-1}$	1087 $\text{cm}^{-1}$
909 $\text{cm}^{-1}$		82.0	81.8
991 $\text{cm}^{-1}$			46.2
1087 $\text{cm}^{-1}$			

Calibration curve of the PLS quantification method with the PI of 96.3 (Figure 23) shows that nine calibration spectra were used to determine the predicted values and two validation spectra were used to validate the calibration set.

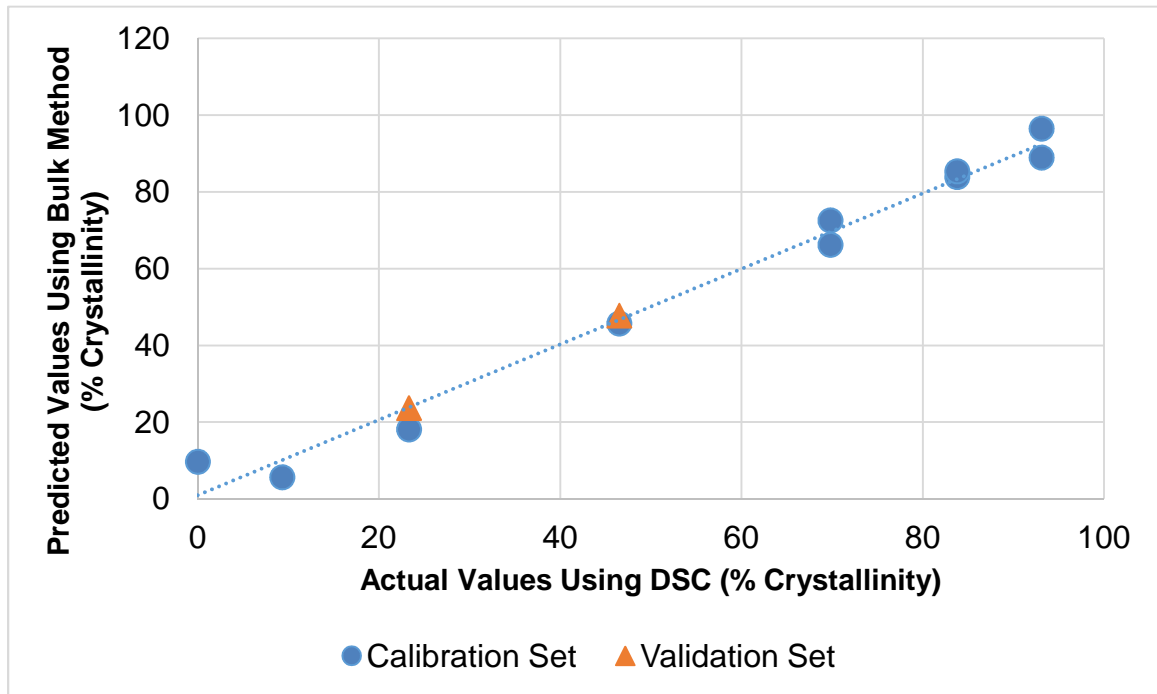


Figure 23: The PLS quantification method calibration curve of 1087, 991, and 909  $\text{cm}^{-1}$  regions. The calibration set were the observations used and the validation set was used to calculate the RMSEP values.

### 3.5. Analysis of Commercialized Cake Mixes

Commercial mixes were measured using the three methods to determine if the bulk method was adequate at measuring the sucrose crystallinity of these samples (Table 11).

Table 11: Baking mix sucrose results determined by AOAC method and % sucrose crystallinity by DSC along with FTIR % sucrose crystallinity results.

Commercial Baking Mix Variations <sup>1</sup>	Sucrose by AOAC 977.20 (%) ± SD	% Sucrose Crystallinity by DSC Method (%) ± SD	% Sucrose Crystallinity by FTIR Bulk Method (%) ± SD
Angel Food Cake	60.1 ± 0.15	61.89 ± 5.8	54.24 ± 3.1
Chocolate Cake	41.3 ± 0.65	38.99 ± 1.2	39.57 ± 0.27
Pound Cake	46.1 ± 1.2	35.19 ± 0.24	48.00 ± 1.6
Red Velvet Cake	39.3 ± 0.10	49.42 ± 0.58	49.55 ± 2.6
White Cake	40.5 ± 0.35	37.44 ± 5.9	51.46 ± 4.6
Yellow Cake	38.1 ± 0.60	40.32 ± 4.2	37.95 ± 0.25

<sup>1</sup>Ingredient declaration information of the cake mixes (Appendix A)

The bulk method predicted values were not statistically different from the values determined by DSC; therefore the quantification by FTIR is feasible as a rapid, non-destructive method to quantify sucrose crystallinity. However, the accuracy of the quantification method on non-carbohydrate products may be limited due to the interfering spectra from non-sucrose constituents. Several factors such as other ingredients in the formula (e.g. fat, grains, and protein) or color (e.g. cocoa) can possibly affect the bulk spectral response.

Previous experimentation to remove confounding spectra such as moisture and particle size has shown to be effective at defining the parameters the FTIR method can perform. To broaden the methodology and increase the robustness, it would be beneficial to continue further refinement of the method to test other sucrose mediums such as fat and protein, along with the effect of color.

This method could be implemented inline with plant production to ensure the proper amount of sucrose is delivered in different mix variations. The carbohydrate rich commercialized mixes did not have interfering spectra and were similar to the samples used to build the quantification curve in texture and particle size.

### 3.6. The Difference between Bulk and Spatial FTIR

FTIR bulk method allowed for a sampling of a larger area which enabled more of the signal to be redirected back to the detector. Food surfaces such as crystalline sucrose had a porous and microscopically, different angled surface. This posed an issue when the FTIR microscope was used, because the incident beam would enter the sample and the diffuse reflectance would occur on a small window of sample. In comparison, the bulk sample reflected back more light back to the detector than the microscope method allowing for lower noise in the sample and less scatter of the light from the larger sample size or aperture (Figure 24).

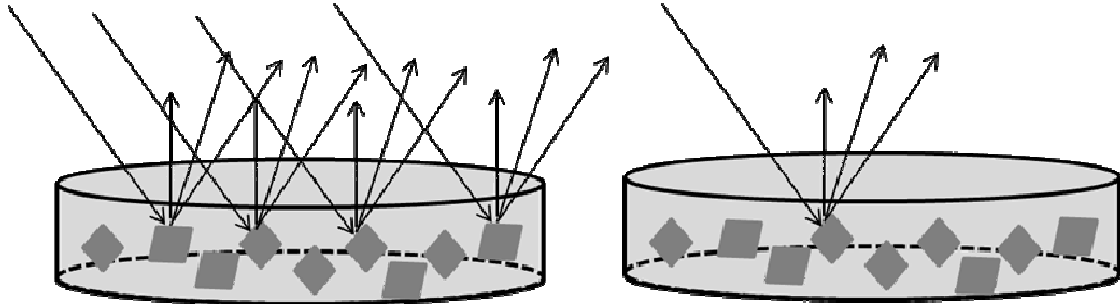


Figure 24: Right side represents the bulk sample measurement where the multiple incidents of light occur along with a larger amount of diffuse reflectance that is reflected back into the detector. The left side represents the FTIR microscope sample measurement where the aperture is smaller and therefore has a smaller amount of light reflected back to the detector.

Depending on the orientation of a sucrose crystal at the specified point the FTIR microscope was aiming at, the reflectance was either more intense back to the detector giving a higher measurement or less intense and noisier giving a lower measurement of percent crystallinity. This difference in intensities changed the

predicted percent crystallinity which caused high variations in the response (Figure 24).

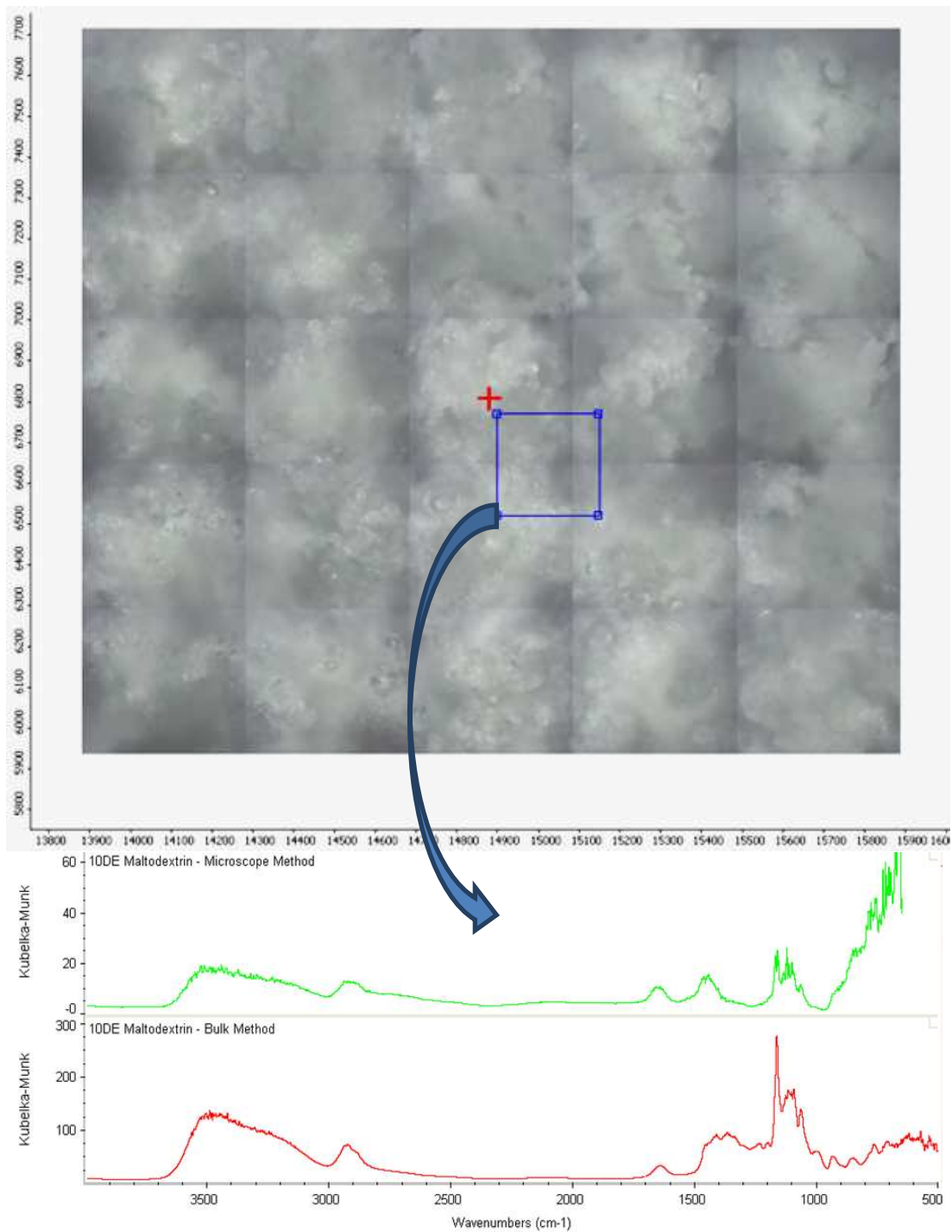


Figure 25: An image of the total surface of 100% 10DE maltodextrin where the location of the 2 x 2 map taken at a (x, y) of approximately (14900 – 15150, 6550 – 6800). Microscope method spectra of a single point in comparison to the bulk method of 100% 10DE maltodextrin

Through the microscope method the powdered 10DE maltodextrin did not show to have different angles which would vary the intensity of the response, but instead it seemed to have a more uniform surface (Figure 25) compared to the 100% sucrose sample (Figure 26).

The spectra from the 10DE maltodextrin and sucrose samples analyzed by the microscope method matched the spectra of controls from the bulk method. Similar patterns in the spectra from both methods showed promise to use the microscope method in the quantification. This also enables spatial differentiation between sucrose and maltodextrin to both visually see differences in the sample, and possibly quantify differences throughout the surface.

Intensity differences between the samples could be from particle size or incident beam intensity differences, but characteristic peaks in the  $1500\text{ cm}^{-1}$  to  $600\text{ cm}^{-1}$  region were analogous to the bulk method. This showed promise to use the FTIR microscope method to quantify for sucrose crystallinity with the method built on the bulk method. The peaks of interest used in the calibration of the PLS quantification method seemed to be mostly undisturbed other than intensity.

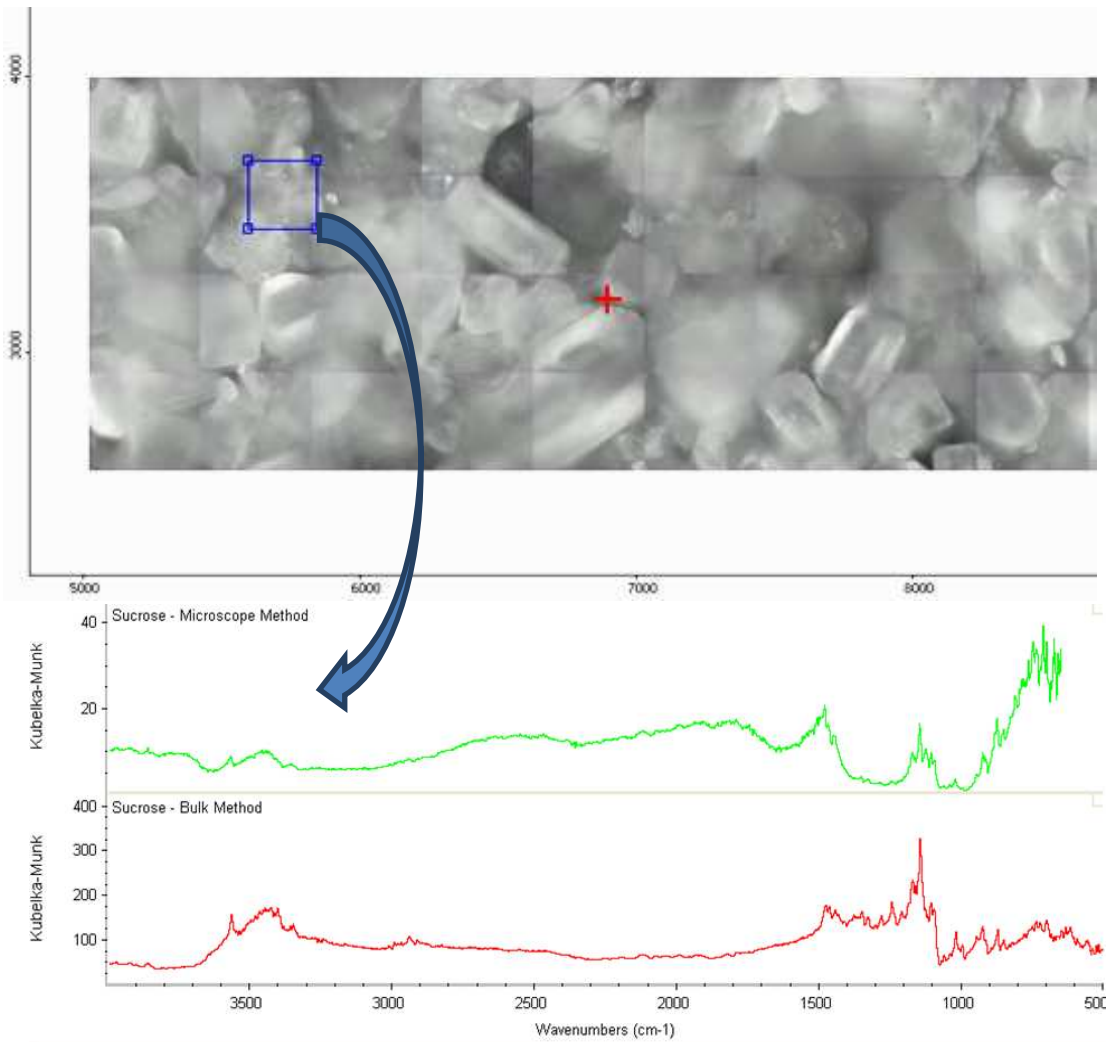


Figure 26: A 100% sucrose sample where the location of the 2 x 2 map taken at a (x, y) of approximately (5500 – 5750, 3500 – 3750). Microscope method spectra of a single point in comparison to the bulk method of sucrose

The 100% sucrose FTIR microscope image (Figure 26) shows the differences in orientation that occurred when sucrose was in the mixture. Creating a uniform surface with sucrose crystals was difficult to achieve which created the variability in the response. The spectra from both the maltodextrin and the sucrose sample had characteristics of the bulk sample spectra. The quality check between a bulk method and the microscope method shows that there is a shift in intensities along with a baseline offset in the microscope method starting around  $900\text{ cm}^{-1}$  which is around the regions used to calibrate the quantification method.

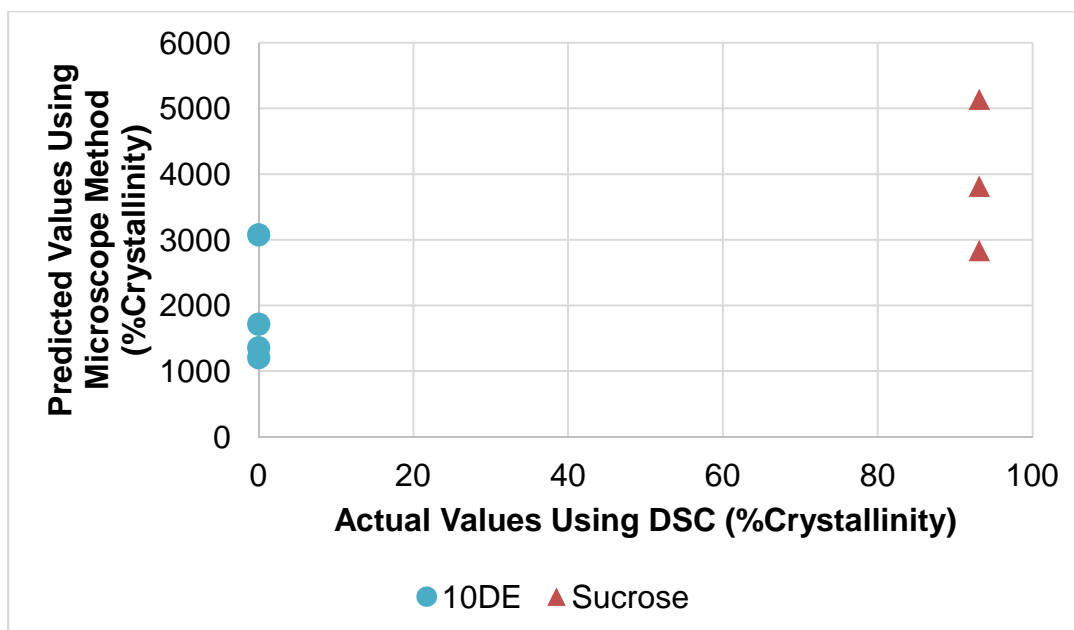


Figure 27: 10DE maltodextrin and sucrose quantified using the FTIR microscope spectra

The large percentages were attributed to the higher incident beam intensity from the FTIR microscope method and the high variability of those values was attributed to the sporadic refraction of light from the surface of the sucrose samples (Figure 27). There is an offset in the quantification method along with a magnitude of difference. This could be from the granulation size, where smaller particle sizes would normalize the response and decrease the overall intensity.



### 3.7. Crystal Size Effect on the FTIR Microscope Image

Analytical grade sucrose particle size changed from a particle size of  $d(0.5)=368.5 \mu\text{m}$  (Figure 28) to  $d(0.5)=96.6 \mu\text{m}$  (Figure 29).

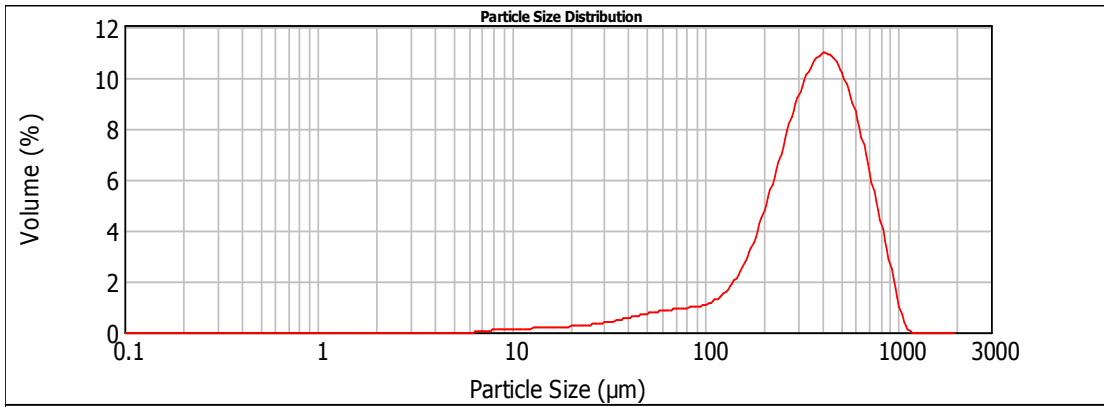


Figure 28: Particle size distribution of analytical grade sucrose with  $d(0.5) = 368.5 \mu\text{m}$

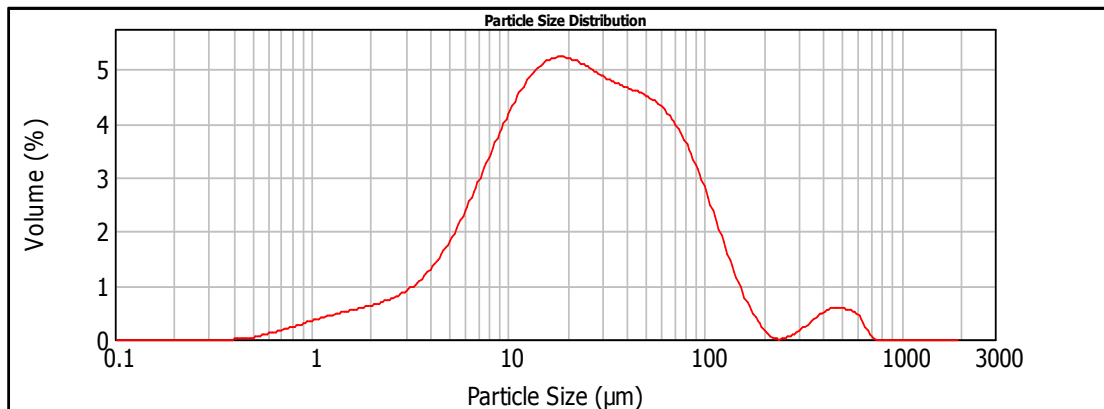


Figure 29: Particle size distribution of powdered sucrose with  $d(0.5) = 96.6 \mu\text{m}$

There was no effect on the image between the powdered sucrose samples and the analytical grade sucrose samples (Figure 30). As shown in the plotted values of the predicted percent crystallinity from the FTIR microscope method, there is no statistical difference between different granulation sizes of sucrose in percent crystallinity. The intensity variability of the analytical grade sucrose was directionally higher than the powdered sucrose sample prediction.

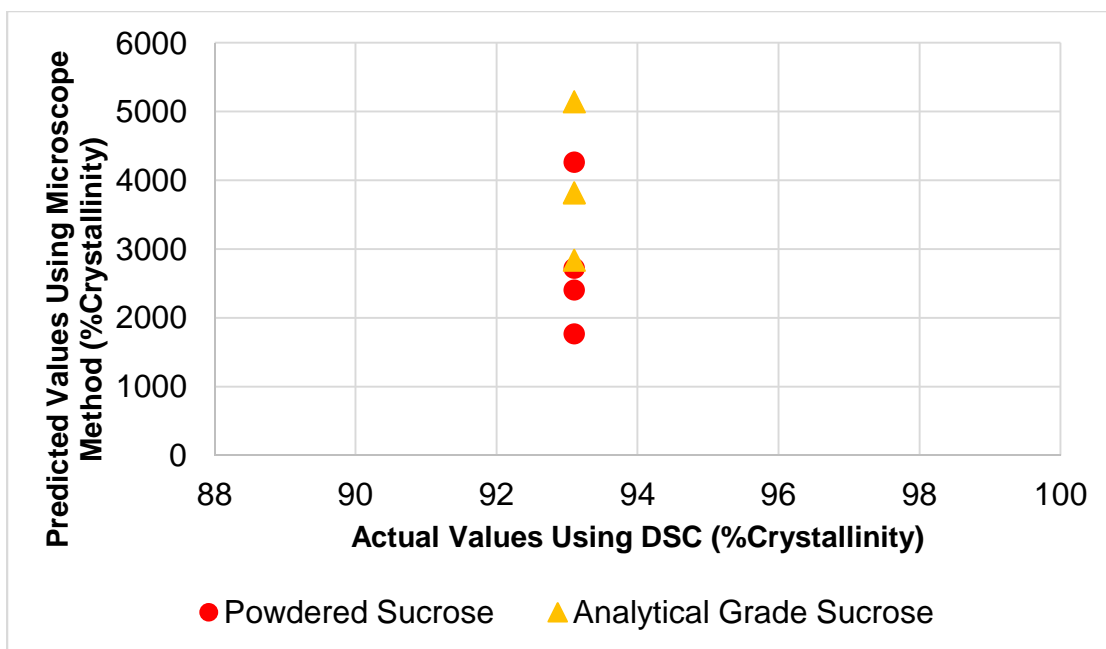


Figure 30: Predicted values of percent crystallinity of powdered and analytical grade sucrose.

### 3.8. Sucrose and 10DE Maltodextrin Mixtures Analyzed by the FTIR Microscope Method

Sucrose crystallinity values had a high range of difference when pure sucrose was analyzed using the FTIR microscope. When the 10DE maltodextrin samples were analyzed, a different result in intensity variability was shown. The sucrose crystals can be differentiated from the maltodextrin powder because of the shape and size of the sucrose. The 100% maltodextrin sample prediction had a range of percent crystallinity values which were magnitudes higher in crystallinity than the bulk method (Figure 30).

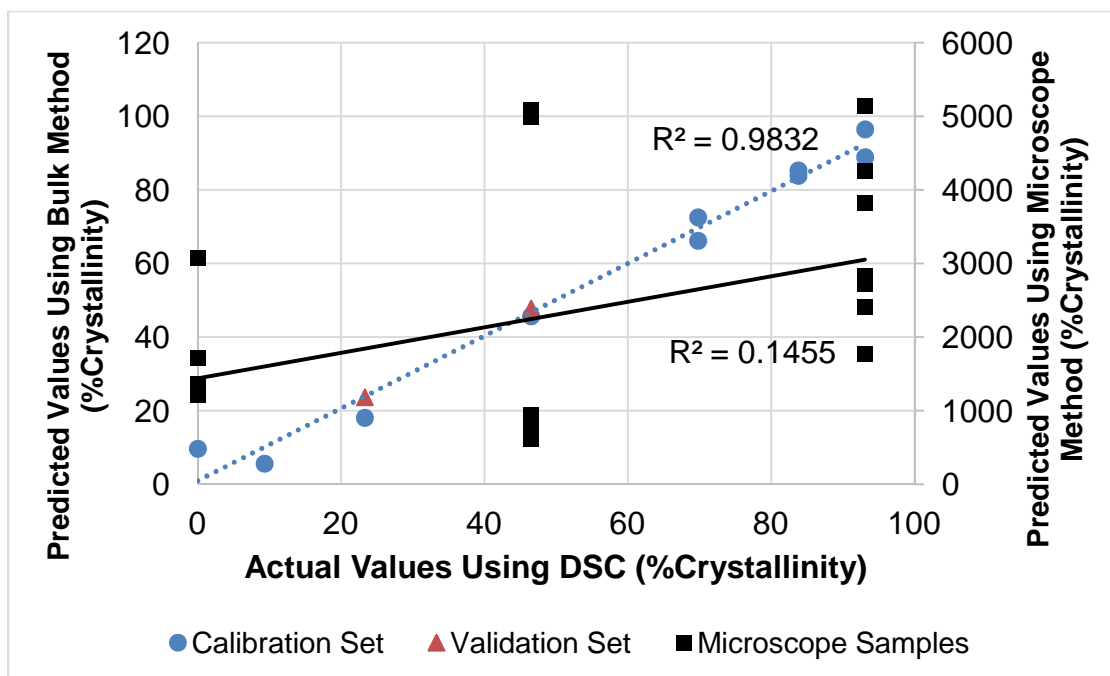


Figure 31: The FTIR microscope samples were plotted to show the regression shift between the bulk method and the microscope method. Also the intensity variability was more pronounced with the sucrose samples than with the maltodextrin samples.

The original regression line of the bulk method which was used to develop the quantification method (Figure 31) is represented with the dashed line  $R^2=0.98$ . The FTIR microscope method regression line is shown as a solid line  $R^2=0.14$ . The shift in regression lines was a confirmation that the microscope method predicted values which were different from the original bulk method. Influences such as the intensity of the beam and refraction from the crystal surface demonstrate the FTIR microscope is a sensitive method and different settings can cause dramatic shifts in response. This method can qualitatively determine sucrose and other constituents spatially, but not quantitatively.

This result validates the FTIR microscope method to be qualitative but is not a feasible quantitative method. The quantification method does not mathematically work with the spectral data that the microscope method produces. The significant

shift in increased percent crystallinity occurs even with samples where no crystallinity would be expected such as the 10DE maltodextrin samples.

#### **4. Conclusions, Implications, and Recommendations**

The FTIR sucrose crystallinity quantification was an effective method to quantify sucrose crystallinity when compared to the DSC and AOAC methods. Further optimization of the method would likely be needed to continue to encompass different non-aqueous matrices including sucrose and other common food components. In bakery mix applications, the bulk quantification method successfully predicted percent sucrose crystallinity compared to the values determined by DSC.

The FTIR microscope spatial method demonstrated that there were differences in the sample, but it was not useful as a quantitative method. This large difference between the two methods was attributed to the energy differences between the bulk method and the spatial method which were a result of sucrose orientation. The feasibility of the FTIR microscope method, or spatial method, was low in model food applications, and does not appear to add to the usefulness of visual microscopy. However, by decreasing magnification and broadening sampling points, it may be possible to use the bulk method in a large scale spatial analysis, such as a FTIR at the end of a dryer in a plant. In addition, other sampling techniques (e.g. probes) should be explored to enable other used of this quantification method.

This method development has been the first step to exploring the use of FTIR to quantify for sucrose crystallinity. Like all methodology development, refinement and additional data processing are needed throughout the development and usage stages of a method. This research enables further technology development to facilitate a more rapid and dynamic approach towards quantifying crystalline sucrose.

## 5. References

- AOAC Official Method 997.20. (2006). [AOAC] *The Association of Analytical Communities (1977). Separations of Sugars in Honey*. Retrieved August 15, 2014, from [http://www.eoma.aoac.org/gateway/readFile.asp?id=977\\_20.pdf](http://www.eoma.aoac.org/gateway/readFile.asp?id=977_20.pdf)
- Archibald, D. D., & Kays, S. E. (2000). Determination of total dietary fiber of intact cereal food products by near-infrared reflectance. *Journal of Agricultural and Food Chemistry*, *48*(10), 4477–4486.
- Beebe, K. R., Pell, R. J., & Seasholtz, M. B. (1998). *Chemometrics: a practical guide* (p. 348). Canada: John Wiley & Sons.
- Ben-Yoseph, E., Hartel, R. W., & Howling, D. (2000). Three-dimensional model of phase transition of thin sucrose films during drying. *Journal of Food Engineering*, *44*(1), 13–22.
- Brereton, R. G. (2007). *Applied Chemometrics for Scientists* (p. 396). West Sussex, England: John Wiley & Sons.
- Brizuela, A., Bichara, L., Romano, E., Yurquina, A., Locatelli, S., & Antonia, S. (2012). A complete characterization of the vibrational spectra of sucrose. *Carbohydrate Research*, *361*, 212–218.
- Bugay, D. E. (2001). Characterization of the solid-state: Spectroscopic techniques. *Advanced Drug Delivery Reviews*, *48*(1), 43–65.
- Chen, J. (2013). *State Behavior of Sucrose and Corn Syrup Mixtures for RTE Cereal Coatings*. University of Wisconsin - Madison.
- Chinachoti, P., & Steinberg, M. P. (1986). Crystallinity of Sucrose by X-ray Diffraction as Influenced by Absorption versus Desorption, Waxy Maize Starch Content, and Water Activity. *Journal of Food Engineering*, *51*(2).
- Cotton, R. H., Rebers, P. A., Maudru, J. E., & Rorabaugh, G. (1955). The Role of Sugar in the Food Industry. In *Uses of Sugars and Other Carbohydrates in the Food Industry* (pp. 3–20). Washington: American Chemical Society.
- Driver, R. D., & Didona, K. (2009). On-Line High-Speed NIR Diffuse-Reflectance Imaging Spectroscopy In Food Quality Monitoring, *7315*, 73150J–73150J–8.
- Gianfrancesco, a., Smarrito-Menzio, C., Niederreiter, G., & Palzer, S. (2012). Developing Supra-Molecular Structures During Freeze-Drying of Food. *Drying Technology*, *30*(11-12), 1160–1166.

- Griffiths, P. R., & Haseth, J. A. De. (2007). *Fourier Transform Infrared Spectrometry* (p. 704). John Wiley & Sons. Retrieved from <http://books.google.com/books?hl=en&lr=&id=ZecrNiUkHToC&pgis=1>
- Hartel, R. W. (2001). *Crystallization in Foods* (p. 325). Gaithersburg, MD: Springer.
- Hartel, R. W., Ergun, R., & Vogel, S. (2011). Phase/State Transitions of Confectionery Sweeteners: Thermodynamic and Kinetic Aspects. *Comprehensive Reviews in Food Science and Food Safety*, 10(1), 17–32.
- Hartel, R. W., & Shastry, A. V. (1991). Sugar crystallization in food products. *Critical Reviews in Food Science and Nutrition*, 30(1), 49–112.
- Hashim, D. M., Man, Y. B. C., Norakasha, R., Shuhaimi, M., Salmah, Y., & Syahariza, Z. A. (2010). Potential use of Fourier transform infrared spectroscopy for differentiation of bovine and porcine gelatins. *Food Chemistry*, 118(3), 856–860.
- Kaláb, M., Allan-Wojtas, P., & Miller, S. S. (1995). Microscopy and other imaging techniques in food structure analysis. *Trends in Food Science & Technology*, 6(6), 177–186.
- Kelly, J. F. D., & Downey, G. (2005). Detection of sugar adulterants in apple juice using fourier transform infrared spectroscopy and chemometrics. *Journal of Agricultural and Food Chemistry*, 53(9), 3281–3286.
- Larkin, P. (2011). Introduction: Infrared and Raman Spectroscopy. In *Infrared and Raman Spectroscopy; Principles and Spectral Interpretation* (pp. 1–5). Waltham, MA: Elsevier.
- Lee, J. W. (2010). *Investigation Of Thermal Decomposition as the Cause of the Loss of Crystalline Structure in Sucrose, Glucose, and Fructose*. University of Illinois at Urbana-Champaign.
- Lee, J. W., Thomas, L. C., Jerrell, J., Feng, H., Cadwallader, K. R., & Schmidt, S. J. (2011). Investigation of thermal decomposition as the kinetic process that causes the loss of crystalline structure in sucrose using a chemical analysis approach (Part II). *Journal of Agricultural and Food Chemistry*, 59(2), 702–712.
- Lee, J. W., Thomas, L. C., & Schmidt, S. J. (2011a). Can the thermodynamic melting temperature of sucrose, glucose, and fructose be measured using

- rapid-scanning differential scanning calorimetry (DSC)? *Journal of Agricultural and Food Chemistry*, 59, 3306–3310.
- Lee, J. W., Thomas, L. C., & Schmidt, S. J. (2011b). Investigation of the heating rate dependency associated with the loss of crystalline structure in sucrose, glucose, and fructose using a thermal analysis approach (Part I). *Journal of Agricultural and Food Chemistry*, 59, 684–701.
- Lehto, V. P., Tenho, M., Vähä-Heikkilä, K., Harjunen, P., Päällysaho, M., & Väliisaari, J. (2006). The comparison of seven different methods to quantify the amorphous content of spray dried lactose. *Powder Technology*, 167(2), 85–93.
- Linstrom, P. J., & Mallard, W. G. (2013). *NIST Chemistry WebBook, NIST Standard Reference Database Number 69*. Gaithersburg, MD, 20899: National Institute of Standards and Technology. Retrieved from <http://webbook.nist.gov>
- Mark, H., & Workman, J. (2010). Chemometrics in Spectroscopy. *Chemometrics in Spectroscopy*, 25(10), 22–31.
- Mathlouthi, M., Hutteau, F., & Angibous, J. F. (1996). Physicochemical properties and vibrational spectra of small carbohydrates in aqueous solution and the role of water in their sweet taste, 56(3), 215–221.
- Muehlethaler, C., Massonnet, G., & Esseiva, P. (2011). The application of chemometrics on Infrared and Raman spectra as a tool for the forensic analysis of paints. *Forensic Science International*, 209(1-3), 173–82.
- Nielsen, S. S. (2010). *Food Analysis. Food Analysis* (p. 602). West Lafayette, IN: Springer.
- Noel, T. R., Parker, R., & Ring, S. G. (2000). Effect of molecular structure and water content on the dielectric relaxation behaviour of amorphous low molecular weight carbohydrates above and below their glass transition. *Carbohydrate Research*, 329, 839–845.
- Nowakowski, C. (2000). *Effect of Corn Syrups on Stability of Amorphous Sugar Products*. University of Wisconsin-Madison.
- Nowakowski, C., & Hartel, R. W. (2002). Moisture Sorption of Amorphous Sugar Products. *Journal of Food Science*, 67(4), 1419–1425.



- Ottenhof, M. A., MacNaughtan, W., & Farhat, I. a. (2003). FTIR study of state and phase transitions of low moisture sucrose and lactose. *Carbohydrate Research*, 338(21), 2195–2202.
- Pellow-Jarman, M. V., Hendra, P. J., & Lehnert, R. J. (1996). The dependence of Raman signal intensity on particle size for crystal powders. *Vibrational Spectroscopy*, 12(2), 257–261.
- Pilc, J., & White, R. (1995). The Application of FTIR-Microscopy to the Analysis of Paint Binders in Easel Paintings. *National Gallery Technical Bulletin*, 16, 73–84.
- Rencher, A. C., & Schaalje, G. B. (2007). *Linear Models in Statistics. Linear Models in Statistics* (pp. 1–672).
- Reuter, A. (2013). *Optimizing Sample Preparation and Scanning Methods for Component Analysis of Raw Milk by Fourier Transform Near Infrared Spectroscopy*. University of Minnesota.
- Roos, Y. (1995). Characterization of food polymers using state diagrams. *Journal of Food Engineering*, 24(3), 339–360.
- Roos, Y. H. (1998). Phase transitions and structure of solid food matrices. *Current Opinion in Colloid & Interface Science*, 3(6), 651–656.
- Seyer, J. J., Luner, P. E., & Kemper, M. S. (2000). Application of diffuse reflectance near-infrared spectroscopy for determination of crystallinity. *Journal of Pharmaceutical Sciences*, 89(10), 1305–1316.
- Sgualdino, G., Aquilano, D., Vaccari, G., Mantovani, G., & Salamone, A. (1998). Growth morphology of sucrose crystals The role of glucose and fructose as habit-modifiers, 192, 290–299.
- Sgualdino, G., Vaccari, G., Mantovani, G., & Aquilano, D. (1996). Implications of crystal growth theories for mass crystallization: Application to crystallization of sucrose. *Progress in Crystal Growth and Characterization of Materials*, 32, 225–245.
- Shah, B., Kakumanu, V. K., & Bansal, A. K. (2006). Review Analytical Techniques for Quantification of Amorphous / Crystalline Phases in Pharmaceutical Solids, 95(8), 1641–1665.

- Slade, L., & Levine, H. (1991). Beyond water activity: recent advances based on an alternative approach to the assessment of food quality and safety. *Critical Reviews in Food Science and Nutrition*, 30, 115–360.
- Smith, E., & Dent, G. (2005). *Modern Raman Spectroscopy – A Practical Approach* (Vol. 5). West Sussex: John Wiley & Sons.
- Smythe, B. (1967). Sucrose crystal growth. I. Rate of crystal growth in pure solutions. *Australian Journal of Chemistry*.
- Socrates, G. (2001). *Infrared and Raman Characteristic Group Frequencies: Tables and Charts* (p. 347). John Wiley & Sons.
- Stefan, D. (2006). *Multi-block relationships in high dimensions*. University of Minnesota.
- Stephenson, G. a., Forbes, R. a., & Reutzel-Edens, S. M. (2001). Characterization of the solid state: Quantitative issues. *Advanced Drug Delivery Reviews*, 48(1), 67–90.
- Thermo Nicolet Corporation. (2001). Introduction to Fourier Transform Infrared Spectrometry. *Thermo Nicolet*.
- Thermo Nicolet Corporation. (2002). FT-IR vs Dispersive Infrared: Theory of Infrared Spectroscopy Instrumentation. *Thermo Nicolet, TN-00128*.
- USDA. (2011). Sugar: World Markets and Trade, 2009–2012.
- USDA. (2014). Proposed Nutrition Facts Label Changes Are Based on Science and Research. *FDA Consumer Health Information*, 1–2.
- Wilson, J. (2014). *WHO-proposed sugar recommendation comes to less than a soda per day*. *CNN*. Retrieved July 26, 2014, from <http://www.cnn.com/2014/03/06/health/who-sugar-guidelines/>
- Wilson, R. H. (1990). Fourier transform mid-infrared spectroscopy for food analysis, 9(4), 127–131.

**Appendix A: Cake Mix Ingredient Information**

Angel Food Cake	Chocolate Cake	Pound Cake	Red Velvet Cake	White Cake	Yellow Cake
Sugar	Enriched Flour	Sugar	Enriched Flour	Enriched Flour	Enriched Flour
Wheat Flour	Sugar	Enriched Flour	Sugar	Sugar	Sugar
Egg White	Corn Syrup	Corn Syrup	Corn Syrup	Corn Syrup	Corn Syrup
Corn Starch	Cocoa	Soybean/Cottonseed Oil	Leavening	Leavening	Leavening
Baking Soda	Leavening	Corn Starch	Cocoa	Soybean/Cottonseed Oil	Soybean/Cottonseed Oil
Citric Acid	Corn Starch	Leavening	Corn Starch	Corn Starch	Corn Starch
Calcium Chloride	Soybean/Cottonseed Oil	Propylene Glycol	Soybean/Cottonseed Oil	Salt	Soybean/Cottonseed Oil
Soy Protein	Propylene Glycol	Salt	Propylene Glycol	Propylene Glycol	Propylene Glycol
Salt	Distilled Monoglycerides	Distilled Monoglycerides	Salt	Nonfat Milk	Salt
Cellulose Gum	Carob Powder	Xanthan Gum	Dicalcium Phosphate	Dextrose	Distilled Monoglycerides
Artificial Flavor	Salt	Dicalcium Phosphate	Sodium Stearoyl Lactylate	Distilled Monoglycerides	Dicalcium Phosphate
Sodium Lauryl Sulfate	Dicalcium Phosphate	Wheat Starch	Red 40	Dicalcium Phosphate	Flavor
	Sodium Stearoyl Lactylate	Flavor	Xanthan Gum	Sodium Stearoyl Lactylate	Sodium Stearoyl Lactylate
	Flavor	Color	Cellulose Gum	Soy Lecithin	Xanthan Gum
	Xanthan Gum	Citric Acid	Flavor	Xanthan Gum	Cellulose Gum
	Cellulose Gum			Cellulose Gum	Yellow 5&6
				Flavor	Nonfat Milk
					Soy Lecithin